Energy Conversion and Management 342 (2025) 120098

Contents lists available at ScienceDirect

Energy Conversion and Management

journal homepage: www.elsevier.com/locate/enconman

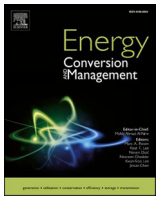

Research Paper

Benefits assessment of a dual-intake-port sliding vane rotary expander replacing the high pressure throttling valve of a *trans*-critical CO_2 refrigeration unit

Fabio Fatigati *, Roberto Cipollone

University of L'Aquila, Department of Industrial and Information Engineering and Economics, Piazzale Ernesto Pontieri, L'Aquila 67100, Italy

ARTICLE INFO

Keywords:
CO_2 refrigeration unit
Energy recovery
Throttling valve replacement
Dual intake port (DIP)
Sliding rotary vane expander (SVRE)

ABSTRACT

Refrigeration sector is responsible of the 7.8 % of the worldwide greenhouse gases emissions pushing participants to COP 28 to commit a reduction close to 70 % by 2050 of the 2022 CO_2 emissions level. To this aim, the adoption of the CO_2 as working fluid is particularly suitable. In refrigeration compression system, to the valve throttling is associated the most severe cycle irreversibility wasting up to the 20 % of compressor input work. To overcome this issue, the replacement of these devices with volumetric expanders is one of the most effective solutions. Despite the huge interest about this topic, a knowledge gap is observed on impact the expander would produce on the refrigeration plant. In fact, the valve replacement with an expander must keep the same cooling performances as well as the same thermodynamic properties on most relevant variables the refrigeration unit had before the substitution. To reach this result, the availability of detailed model of the refrigeration unit is needed, able to represent the whole complexity of the processes occurring (propagative, inertial and volumetric properties). To fill this gap, in the present paper a novel comprehensive model of the unit was developed and experimentally validated against experimental data collected on a fully instrumented test bench in which an industrial refrigeration unit (18 kW as refrigeration power) was operated. Once the model resulted validated, it was used to predict the plant behaviour if the throttling valve was replaced by a Sliding Rotary Vane Expander (SVRE). Concerning the expander design, a further innovation was considered referring to a dual intake port technology DIP. To assess the introduced benefits, an expander model validated in previous works developed by the authors was used. Adapting this model for the application at hand and integrating it with the plant whole model, it was found that an improve up to 20 % the whole efficiency with respect to the baseline case was achieved for the maximum considered external temperature (31 °C-33 °C).

1. Introduction

Refrigeration sector is responsible of the 7.8 % of the worldwide greenhouse gases emissions [1], representing up to 10 % of the whole energy consumption, [2] which is predicted to grow almost tenfold by 2050, [3]. Hence, considering that COP 28 sets the objective of the achievement carbon neutrality by 2050, a transition towards low carbon emissions is needed, [4]. Particularly critical from the energy demand point of view is the refrigeration of supermarkets which severely affects the annual energy demand which reaches peaks of 3–4 % of the year electricity usage in development countries, [5]. Moreover, energy demand for refrigeration is predicted to increase tenfold by 2050, [6].

For this reason, it is fundamental to the develop the technologies and plant configurations ensuring to optimize the refrigeration units, thus reducing the related emissions of this sector, [7].

In this context, CO_2 refrigeration units appear as a promising solution to achieve carbon neutrality objectives [8] considering the naturality of the working fluid. Moreover, the adoption of this fluid ensures a low Global Warming Potential (GWP) which is compliant to the Montreal protocol and Kigali Amendment which introduced restrictions in the usage of high-GWP fluids, [9]. Conventional working fluids present, indeed, high GWP and Ozone Depletion Potential (ODP), [10]. Hence, CO_2 thanks to its advantages in terms of ODP and GWP, non-toxicity, high volumetric cooling capacity and non-flammability, is a real candidate to replace the conventional refrigerants, [11].

These reasons explain the wide interest and the significant growth of the installation of *trans*-critical CO_2 refrigeration units in these last

* Corresponding author.
E-mail address: fabio.fatigati@univaq.it (F. Fatigati).

https://doi.org/10.1016/j.enconman.2025.120098
Received 1 April 2025; Received in revised form 17 June 2025; Accepted 17 June 2025
Available online 20 June 2025

Nomenclature

Symbols

A	cross sectional area [m^2]
A_s	is the heat transfer area [m^2]
c_p	specific thermal capacity of metallic masses [kJ/KgK]
C_d	is the discharge coefficient
C_f	Fanning friction factor
D	pipe diameter [mm]
dx	length of mass element in the flow direction [m]
dp	pressure differential across x [m]
e	total specific internal energy [J/kg]
H	Total specific enthalpy [J/kg]
h_{in}	Expander inlet specific enthalpy [J/kg]
$h_{out,is}$	Expander outlet specific enthalpy in case of isentropic expansion [J/kg]
i	index of chamber
K_p	the pressure loss coefficient
m	mass [kg/s]
$\dot{m}$	Mass flow rate entering exiting boundary volume [kg/s]
$\dot{m}_{CO2}$	CO_2 mass flow rate downstream HPV (total) [kg/s]
$\dot{m}_{liq}$	mass flow rate of liquid phase to evaporators [kg/s]
$\dot{m}_{vap}$	mass flow rate of vapor phase to Flash gas valve [kg/s]
N	population of experimental values
N_v	number of chambers
$P_{ad,is}$	Adiabatic isentropic power [W]
p	fluid pressure [Pa]
$p_{1,total}$	is the total pressure upstream the valve [Pa], [bar]
$p_{2,static}$	the static pressure downstream the valve [Pa], [bar]
P_{ind}	Indicated power [W]
p_i	chamber pressure of the i-chamber [Pa]
P_{mech}	Mechanical power [W]
$P_{mech.loss}$	Mechanical power lost due to friction [W]
$P_{th,Compr}$	Compressor power consumption [kW]
$P_{th,Evaps}$	Cooling load at evaporators [kW]
Q_1	thermal power provided by the fluid 1 to the metallic masses [kW]
Q_2	thermal power provided by the metallic masses to the fluid 2 [kW]
q	vapor quality
T_{fluid}	the temperature of the fluid [K]
T_{wall}	the temperature of the metallic masses [K]
t	the time independent variable [s]
t_{cycle}	time cycle [s]
V	volume of the metallic masses [m^3]
V_i	volume of the i-chamber [m^3]
u	velocity at the boundary [m/s]
V_{int}	expander volume at intake end [m^3]
x	predicted quantity
$\check{x}_i$	measured quantity

Acronyms

COP	Coefficient of Performance
EPV	electric valve
DIP	Dual Intake Port
FGV	Flash Gas valve
HPV	High pressure valve
MD	Maximum absolute Absolute Error
MD_r	Maximum relative absolute Absolute Error
PS	Phase separator tank
RMSE	Root Mean Square Error
$RMSE_r$	Relative Root Mean Square Error
SIP	Single Intake Port
SVRE	Sliding Rotary Vane Expander

Greek letters

α	heat transfer coefficient [W/m^2K]
ΔT	is the effective temperature difference between the fluid and the metallic masses [K]
η_{fluid}	fluid dynamic efficiency
η_{glob}	global efficiency
η_{mech}	mechanical efficiency
η_{vol}	volumetric efficiency
ρ	density of the metallic masses [kg/m^3]
ρ_{int}	Density of CO_2 at expander intake end [kg/m^3]
ω_{exp}	expander speed [RPM]

years, [12]. Nevertheless, in single and two stage *trans*-critical CO_2 refrigeration units the large difference between the inlet and outlet pressure of high pressure expansion valve (HPV) leads to significant throttling losses leading to low Coefficient of Performance, [13]. This involves that significant effort was performed in the recent year to improve the CO_2 refrigeration cycle performance, [14].

The most part of cycle irreversibility is due to throttling valve wasting up to 20 % of the compressor input work, [15]. Hence, among the possible improvements in plant layout and architecture to be efficient and reducing energy consumption and relative CO_2 emissions [16], the replacement of throttling valve with ejectors or expanders is one of the most interesting and attractive solutions, [6]. The introduction of ejectors ensures to recover expansion work [17] and increase the compressor suction pressure, [18] increasing cycle performance, [19]. The use of an expander ensures to achieve a direct energy recovery guaranteeing a higher cooling capacity with respect to the ejector case, [15]. Indeed, when an ejector was used, the pressure reduction of working fluid leads to an increase of flow velocity due to the conservation of the energy. This produces a higher compressor suction pressure thus reducing the compressor power. The introduction of the expander produces a direct recovery converting the thermodynamic energy in shaft power. Hence, due to the more isentropic nature of the expansion process in the expander a larger cooling capacity can be achieved.

In recent year, many study focuses on the expander introduction in compression refrigeration plant. In [20] a three stage piston expander working at near isothermal condition was considered. In [21] a radial piston expander derived from a hydraulic motor was developed finding a potential COP improvement of 7.4 %. Screw expander was also considered in CO_2 refrigeration system. In [22] a CFD study was conducted to evaluate the effect of the injection of oil to seal, lubricate and cool the high pressure gas observing a reduction of 20 % on radial loads. In [22] it was seen that adopting a screw expander at a speed of 3000 RPM, a volumetric efficiency and output power respectively equal to 88.5 % and 3.37 kW can be achieved. Also Scroll expander are considered.

The operation of the expander, unfortunately, severely affects the operating conditions of the refrigerating unit because, if not properly controlled, it modifies the thermodynamics and fluid dynamics of the unit, changing the pressure levels of the evaporators and other main relevant quantities. Its operation, moreover, is challenging considering that the expansion usually produces a two-phases flow, the operation pressure range is unconventional and modified by the flow rate, [20]. All these aspects are the reasons for the strong deviation of the real performances from the predicted ones. New technological solutions are expected from the huge effort observed in literature about the development of two-phase expander, [8]. Apart from the mechanical design of the component which still deserve attention (high pressure operating conditions, mechanical stresses of the blades, wear at tip blades, surface

mechanical damages at the mechanical contacts between moving components, etc…), an eventual reduction of the influence between the upstream–downstream pressure difference and flow rate would be particularly suitable as well as an easy control variable of these two quantities.

In literature, both dynamic and volumetric expander devices were considered. Radial and axial dynamic machines are rarely adopted in small scale applications (0.2 kW-20 kW) due to the rotational speed, sealing and vibration, [20]. Hence, volumetric machines seem to be the best candidates for these applications.

Indeed, in recent year, many study focuses on the expander introduction in compression refrigeration plant. Piston expander presents a higher intake volume which represents an advantage with respect to other volumetric devices, anyway, leakages and machine complexity lead to an efficiency lower than 50 %, [21]. In [22] a three-stage piston expander working at near isothermal condition was considered. In [23] a radial piston expander derived from a hydraulic motor was developed finding a potential COP improvement of 7.4 %. Screw expander was also considered in CO_2 refrigeration system. In [24] it was seen that adopting a screw expander at a speed of 3000 RPM, a volumetric efficiency and output power respectively equal to 88.5 % and 3.37 kW can be achieved. In [25] a CFD study was conducted to evaluate the effect of the injection of oil to seal, lubricate and cool the high pressure gas observing a reduction of 20 % on radial loads. Scroll expander is a feasible solution even if it is usually realized from a reversed compressor, [26], without a specific design attention. In [27] a scroll expander with an inlet volume of 2.8 cm^3 was built obtaining that the best pressure ratio was equal to 1.95 while the best performance (83 % of isentropic efficiency) is achieved for a speed between 2200 RPM and 3400 RPM. In [28] it was seen that larger orbiting radii and shaft bearing allow to improve isentropic efficiency.

Among all the technological alternatives, Sliding Vane Rotary Expanders (SVRE) appear as a very attractive solution due to high reliability, compactness, ease of manufacture and low cost, [29], despite they present greater mechanical and volumetric losses with respect to other volumetric devices.

In [30] it was seen as friction losses have a major impact on the whole performance than volumetric losses in two phase and supercritical region. The adoption of springs inside the rotor slots allows the increase the centrifugal force which pushes the blade outside it, improving isentropic and volumetric efficiency respectively by 30 % and 60 %, [31]. Further improvement to boost the expander efficiency are the adoption of greater eccentricity and a blade inclination, [32]. Similar positive results are presented in [33] where an increase of the volumetric and isentropic efficiencies is close to 30 % and 23 % respectively. To reduce the clearance gap between stator inner surface and blades tip, in [34] high pressure working fluid is recirculated under the blades to increase the pushing action on the blades. In this way, a COP increase up to 27 % replacing the throttling valve. In [35], the COP increase was in the order of 22 % mainly depending on the condensation temperature and subcooling degree at expander inlet. The introduction of a volumetric expander to replace throttling valve is economically feasible as demonstrated in [36], observing a payback period less than 5 years for a machine with a global efficiency up to 50 %.

Despite the high interest in literature, some issues and challenges remain open, [37], together those already mentioned. Particularly important is the aspect related to the operation in off design conditions [37] and how the expander modifies the refrigerating performances of the unit, i.e., definitively the paying factor (cold thermal power). As already mentioned, this calls for the development of design techniques ensuring to control the expander impact on the whole plant behavior. This could open the way to a huge retrofitting activity of the existing units already in operation. What is more, expanders conceived for these applications present too low volumetric efficiency in the order of 35 %–40 % which severely affects the whole performance, [34]. An improvement in this sense leads to a higher energy recovery and consequently to larger benefits in terms of COP.

Therefore, to contribute to fill these knowledge gaps, a comprehensive and physical model of the refrigeration unit was developed. The novel aspect of the model is that it is not only a thermodynamic type (as it is usual in the sector) but able to represent the real layout of the unit with its capacitive, inertial and propagative properties. This represents a novelty as the sector is rich of thermodynamic model of CO_2 *trans*-critical refrigeration unit model but to the authors best knowledge propagative and capacitive model are absent. In [38] a numerical dynamic model of a CO2 refrigeration system was presented but oriented to the analysis of multiple configurations not considering the integration with expander model. In [39] a detailed theoretical model was developed but focusing on steady state analysis and not considering the expander installation. A one-dimensional thermodynamic model was developed in [40] but focusing on the introduction of the ejector instead of the expander.

A peculiarity of the proposed model is that the piping layout and volumes (reservoir and those of the fluid passages in the heat exchanger) are considered to ensure a more accurate prediction of dynamic and off design performance. Moreover, the accuracy and the capability of the model are assessed thanks to a deep experimental validation carried out against data collected on a commercial CO_2 *trans*-critical unit of a rated cooling power of 18 kW, produced by the EPTA Refrigeration Group fully instrumented to assess its behavior in [41]. Thanks to the model, the effect of the replacement of HPV with a Sliding Rotary Vane Expander (SVRE) can be predicted and taken into account in the expander design.

Indeed, the design of the expander involved has been also done defining its intake volume which represents the starting and the most important point. Using a refined physically consistent model of it developed by the authors in previous works [42,43] the other design aspects were designed, reaching a geometrical representation of the expander. Considering the high reproducibility produced by the model when compared with experimental data, [43], it has been integrated into the model of the refrigeration unit. The effects it produces on the operating conditions of the refrigeration unit have been predicted with a high level of confidence, considering that the two parts (refrigerating unit and expander) were successfully compared with experimental data. A comparison between the originally equipped unit (with a HPV) and that modified by the presence of the expander has been discussed. Main conclusion it that the expander can be seen as a revolving valve, affecting the permeability of the unit, defined as the ratio between the plant maximum pressure and working fluid mass flow rate circulating in the unit. Its speed of rotation modifies the “rotating valve behavior from a thermodynamic point of view”. So, the expander speed of rotation resulted a very effective variable to restore the original thermodynamic performances of the refrigeration unit.

To increase the power recovered by the expander (instead of wasting energy inside a HPV), a new concept of it has been considered developed by the authors in previous works, [42,43]. The so-called Dual Intake Port (DIP) technology is considered consisting in an additional intake port opening after the closure of the main one. In previous works, [42,43], the authors experimentally and theoretically demonstrated that this solution has a twofold benefit when applied in Organic Rankine Cycle-based unit: (1) an increase in the permeability of the plant for the same mass flow rate crossing the expander, i.e. the reduction of its intake pressure, (2) the increase of the flow rate crossing the expander when the pressure difference remains constant, i.e., the increase of the power produced. Hence, considering the suitability of this technology for SVRE, authors demonstrated that, through the integration of an expander based on a DIP technology on a refrigerating unit, a significant COP increase was obtained. This is particularly suitable considering that the refrigerating unit used CO_2 as operating fluid, usually characterized by COP values lower than the units operating with more conventional fluids, mainly at high environmental temperatures.

2. Material and methods

2.1. Trans-critical CO_2 refrigeration unit and experimental test bench

The reference CO_2 *trans*-critical refrigeration unit considered in this work was reported in Fig. 1 whereas its layout was shown in Fig. 2. The unit corresponds to a commercial device produced by EPTA refrigeration Group which has been extensively monitored to have a complete experimental characterization of the thermal and fluid dynamical properties.

As Fig. 2 shows, (a) and (b) are two equivalent evaporators operating in parallel having split the mass flow rate, the maximum extracted thermal power (cooling load) is of 18 kWt. Evaporators are two plate heat exchangers SWEP – B9Hx32/1P. In the experimental facility, the cold source is represented by a mixture of water and glycol to simulate the real one represented by the air of the environment that must be cooled.

The working fluid circulating inside the plant (CO_2) is compressed through a BITZER 4JTC – 15 K piston alternative compressor (c) of a rated power of 17 kW_e, [44]. The unit adopts also a back-up equivalent piston operating in parallel. In Table 1 the main features of compressors are reported.

The thermal power is released to the hot source (represented by the external air) through a LUVE EAV5N 5311 gas cooler (d) whose main properties are reported in Table 2. Leaving gas cooler, the working fluid then enters a Danfoss ICMTS 20° High Pressure Valve (HPV) where a lamination isenthalpic transformation happens involving the fluids decreasing from a maximum pressure (75 bar) up to the intermediate pressure level (35 bar).

The refrigeration fluid is gathered in a Phase Separator (PS) tank of 110 L (f) thus separating the vapor and liquid phase. The liquid phase enters a Carel EEV valve (g) and flows towards evaporators where evaporating pressure is in the order of 26–28. The vapor phase is instead provided to a Flash Gas Valve EPV valve Carel E3V45 (h) allowing that working fluid expands up to the pressure of the working fluid at the evaporator outlet (26 bar). The two streams are rejoined in a collector where the vapor was aspirated by compressor.

The experimental test bench ensures to measure the following quantities:

a) CO_2 inlet and outlet temperature at the dry cooler;
b) Water temperature at evaporators inlet;
c) Water temperature at evaporators outlet;
d) Water flow rate;
e) Total CO_2 flow rate;
f) CO_2 flow rate, temperatures and pressures at the evaporators;
g) CO_2 pressure and temperature at compressor inlet and outlet.

Concerning a-d quantities, they are handled through a proprietary acquisition system built on the platform DAQ Agilent 34901A. The remaining quantities are instead measured via the platform Boss/Carel present on the unit. The control system pRack300T allows to modify the opening rate of valves and compressor operating conditions.

Measurement uncertainties are assessed according to the approach reported in Eq. (1):

$$Y = \sqrt{\sum_{i=1}^{N} \left(\frac{\partial y}{\partial x_i}\right)^2 X_i^2} \quad (1)$$

where:Y is the absolute uncertainty of the y quantity depending on i-quantityxi whose absolute efficiency is XiN is the number of quantities on which Y depends.

It is worth mentioning that in Fig. 2(b) the *trans*-critical CO_2 unit with expander was reported, the difference with respect to the baseline case is that SVRE is introduced instead of HPV valve (e).

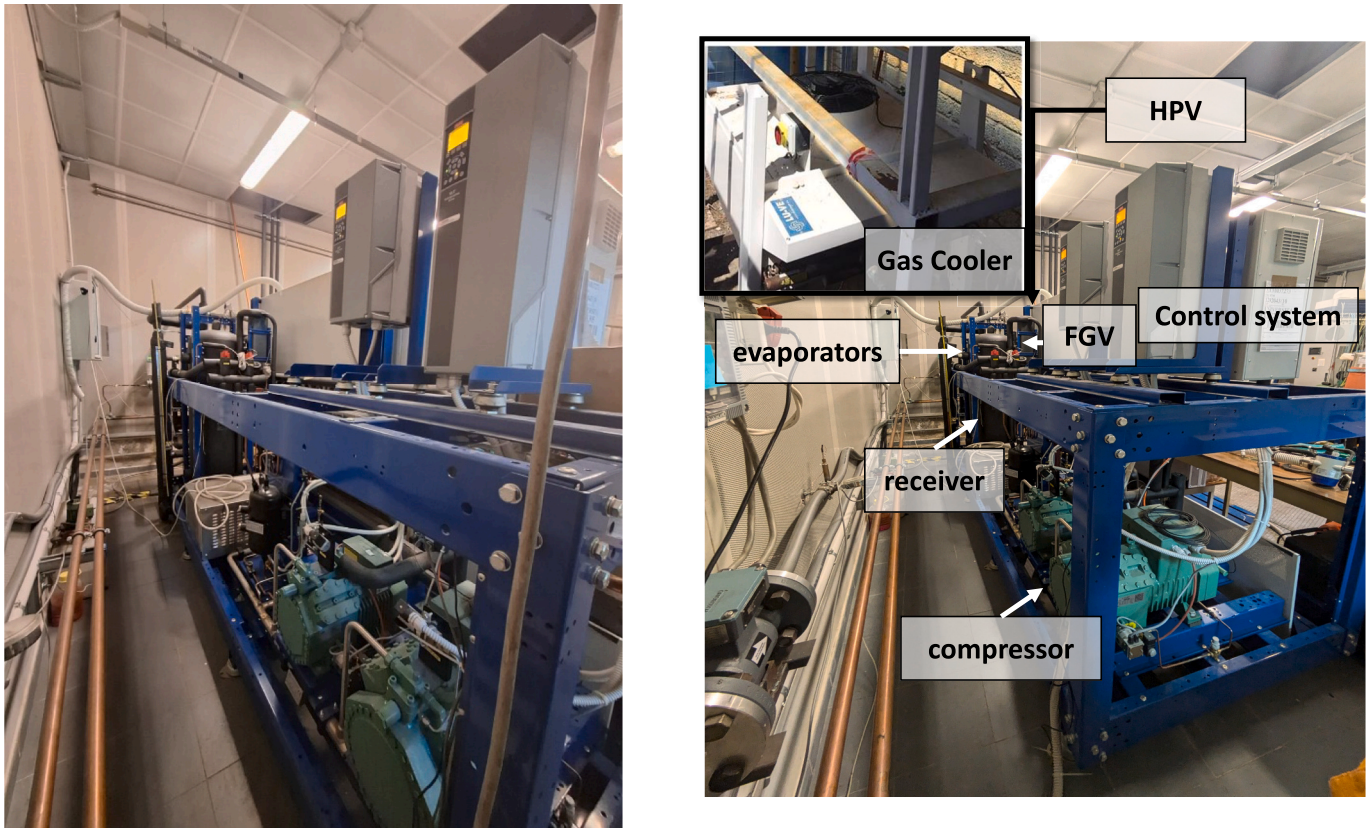

Fig. 1. Trans-critical CO_2 refrigeration unit.

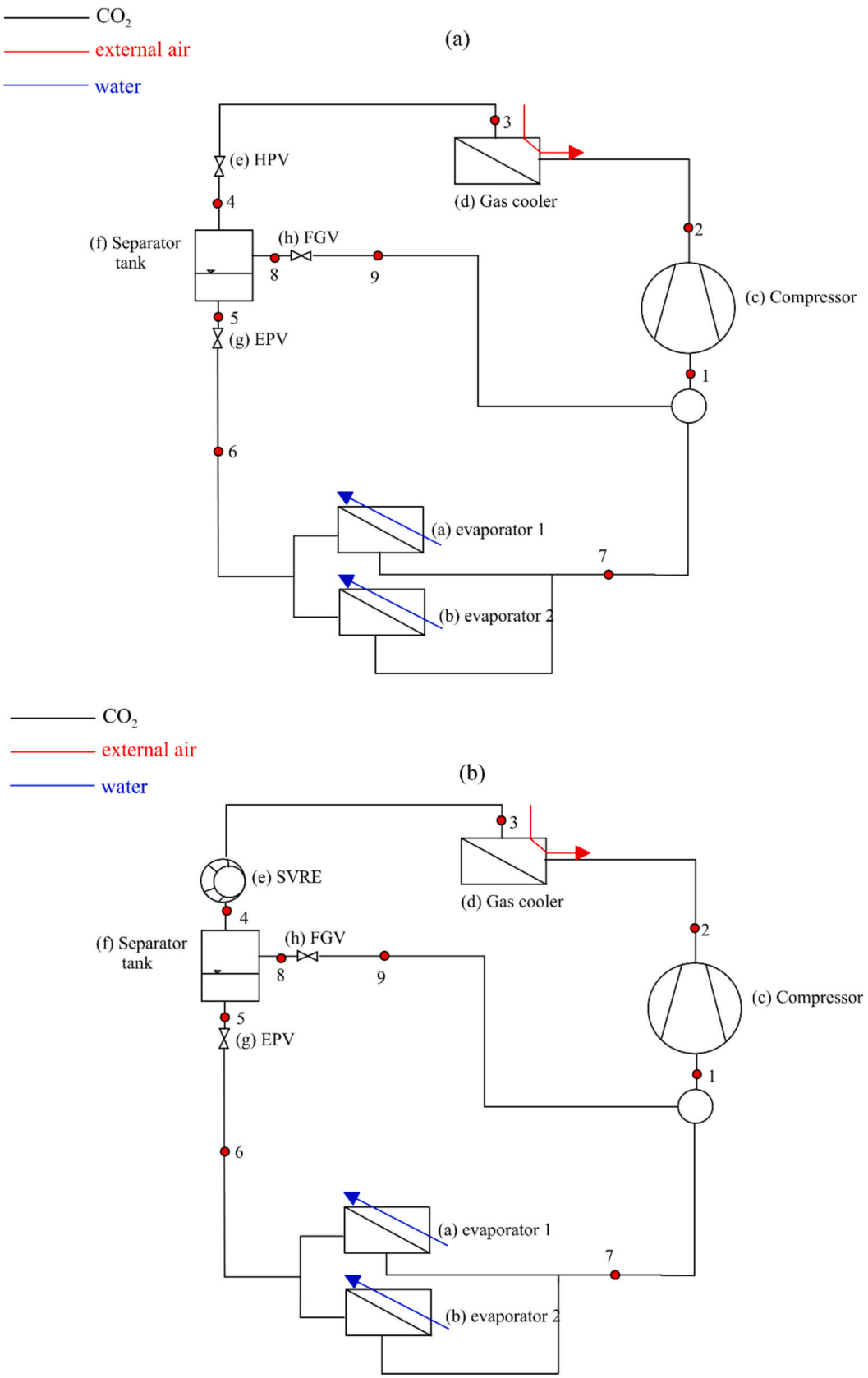

Fig. 2. Baseline transcritical CO_2 refrigeration unit (a) and plant layout with expander replacing the HPV valve (b).

Table 1
Compressor specs.

Displaced volume	105 cm3
Maximum operating pressure	160 bar
Maximum power absorbed	17.7 kW
Oil charge	2.6 L
Oil type	BSE85K

Table 2
Gas Cooler specs.

Power size	29,3–32.9 kW
Flow rate	6400–7600 m3/h
Electric power absorption	400–600 W
Volume	10 Liters
External surface	56.5 m^2
Internal surface	7.4 m^2

2.2. Theoretical model

The plant theoretical model was developed in GT-Suite environment adopting an integrated zero and mono dimensional 0D-1D thermo-fluid-dynamic analysis approach. In this way, piping and heat exchangers express the three fluid dynamics properties (capacitive, inertial and propagative), reservoirs only one (capacitive). The reciprocating compressor is modelled through a characteristic map based on the experimental values collected and those provided by manufacturer, [38].

In Fig. 3 the model of the unit is reported.

The 1-D thermo-fluid-dynamic approach requires the discretization of the pipes of the system in multiple sub-elements for each of them the Navier Stokes equation system expressing the mass, momentum and energy conservation (equations (2.1), 2.2 and 2.3) are solved through an implicit method.

$$\frac{dm}{dt} = \sum_{boundaries} \dot{m}_{in} \tag{2.1}$$

$$\frac{d(\rho HV)}{dt} = \sum_{boundaries} (\dot{m}H) + V\frac{dp}{dt} - \alpha A_s(T_{fluid} - T_{wall}) \tag{2.2}$$

$$\frac{d\dot{m}}{dt} = \frac{dpA + \sum_{boundaries}(\dot{m}u) - 4C_f\frac{\rho u|u|dxA}{D} - K_p\left(\frac{\rho u|u|}{2}\right)A}{dx} \tag{2.3}$$

where:$\dot{m}$ is the mass flow rate entering (+) and exiting (−1) the boundary volume, m is mass of the volume, V is the fluid volume, P is fluid pressure, ρ is the fluid density, A is the cross-sectional flow area, A_s is the heat transfer surface area, e is total specific internal energy (internal energy plus kinetic energy per unit mass), H is the total specific enthalpy, α is the heat transfer coefficient, T_{fluid} is the fluid temperature, T_{wall} is the wall temperatureu is the velocity at the boundary, C_f is the Fanning friction factor, K_p is the pressure loss coefficient (commonly due to bend, taper or restriction), D is the equivalent diameter, dx length of mass element in the flow direction (discretization length), dp pressure differential acting across dx.

Concerning the transient analyses, it can be done as well as predicted the behavior at off design. Hence, the real piping layout has been reproduced as it is in reality (according to Fig. 3), thus assessing the distributed and located pressure losses with a high accuracy. Concerning evaporators (a and b) and gas cooler (d) they are modelled according to a set of flow volume and thermal masses as can be seen in Fig. 4. Such

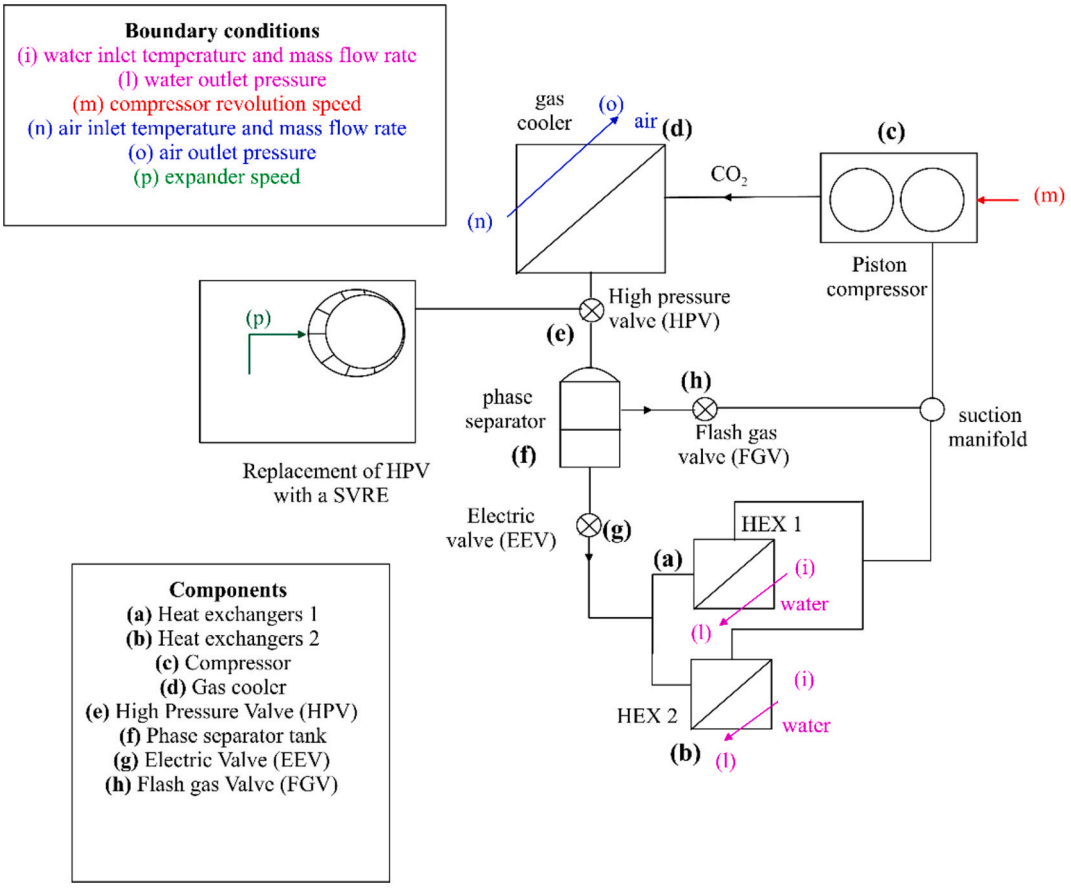

Fig. 3. Theoretical model of the refrigeration unit.

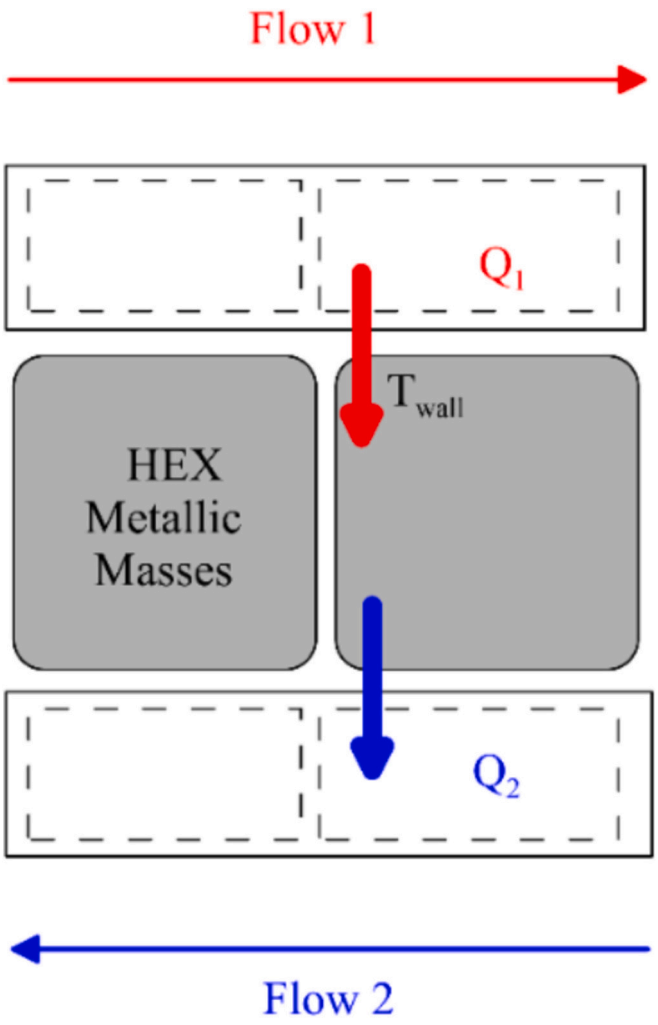

Fig. 4. 1-D Analysis for heat exchangers.

components are treated by adopting the Master/Slave approach. Master section represents the heat transfer between the heat exchanger wall and the working fluid mass flow rate (CO_2). Slave section represents instead the heat transfer between the high and low thermal source and the heat exchanger masses. In Master section the geometry and the correlation to define the heat transfer coefficient reported in Table 3. Fig. 4 shows a scheme of the theoretical approach followed to characterize the dynamic behavior of heat exchangers. According to this approach, the metallic masses of each heat exchangers are discretized in sub-volumes whose sides are in contact with fluid 1 and fluid 2. In this way, it is possible to consider the thermal inertia of HEX metallic masses and the conducive capacity as reported in Eq. (3).

$$\frac{dT_{wall}}{dt} = \frac{Q_1 + Q_2}{\rho V c_p} = \frac{(\alpha A_s \Delta T)_1 + (\alpha A_s \Delta T)_2}{\rho V c_p} \tag{3}$$

In Eq. (1), Q_1 and Q_2 are the thermal power provided by the fluid 1 to the metallic masses (considered positive) and thermal power provided by the metallic masses to Fluid 2 (considered negative). Concerning ρ, V and c_p they are the density, volume and specific thermal capacity of metallic masses, respectively. The heat transfer coefficient is denoted as α and measured in [W/m^2K] whereas A_s is the heat transfer area while ΔT is the effective temperature difference the metallic masses and working fluids.

Hence, as Fig. 4 and Eq. (1) shows, the temperature of metallic masses (T_{wall}) is defined by the thermal power balance between HEX and the two fluids (Fluid 1 and Fluid 2).

In Eq. (1), Q_1 and Q_2 are the thermal power provided by the fluid 1 to the metallic masses (considered positive) and thermal power provided by the metallic masses to Fluid 2 (considered negative). Concerning ρ, V and cp they are the density, volume and specific thermal capacity of metallic masses, respectively. The heat transfer coefficient is denoted as α and measured in [W/m^2K] whereas A is the heat transfer area while ΔT is the effective temperature difference the metallic masses and working fluids.

Hence, as Fig. 4 and Eq. (1) shows, the temperature of metallic masses (T_{wall}) is defined by the thermal power balance between HEX and the two fluids (Fluid 1 and Fluid 2).

It is worth noting that heat transfer coefficient α is are predicted thanks to the empirical correlations. In particular:

Heat transfer coefficients are predicted thanks to the following empirical correlation:

- Heat transfer coefficient for single phase (liquid and vapor) and for supercritical phase with Dittus Boelter [45] correlation.
- Heat transfer coefficient for single phase (liquid and vapor) and for supercritical phase two phase condensation and evaporation with Specific Shah correlations [46].

Throttling valves (HPV, FGV, EEV) produce a significant effect on the behavior of the whole plant, they are modelled as restrictions caused by an orifice with an externally set diameter and the relation which correlates the mass flow rate and pressure drop at valve sides are reported in Eq. (4).

$$\dot{m}_{CO_2} = C_d \rho \left(\frac{\pi D^2}{4}\right) \sqrt{\frac{2(p_{1,total} - p_{2,static})}{\rho}} \tag{4}$$

where: Cd is the discharge coefficient defined according to the approach of Litchatrowicz et al. [47], ρ is the CO_2 density, D the orifice diameter, $p_{1,total}$ is the total pressure upstream the valve and $p_{2,static}$ the static pressure downstream the valve.valve opening rate ϕ defined as as the ratio between the effective valve flow passage area and the maximum one characterized by a circular area whose diameter is equal to D.

For the case at hand, a ϕ equal to 35 % is considered for HPV and 25 % for FGV. The EEV valve is considered totally open (ϕ = 100 %).

Phase separator (PS) is an insulated tank in which the two-phase working fluid leaving the High Pressure valve ($\dot{m}_{CO_2}$) enters. Here, the vapour and liquid phases are separated with the liquid gathered on the bottoming and provided to the evaporator ($\dot{m}_{liq}$) and the vapour ($\dot{m}_{vap}$) taken from above and forwarder to flash gas valve. A scheme of Phase separator model can be seen in Fig. 5. This component is treated by a lumped element to which the mass (2.1), momentum (2.2) and energy conservation Eq. (2.3) can be applied. Mass conservation equation can be particularized as in Eq. (5):

$$\dot{m}_{CO_2} = \dot{m}_{vap} + \dot{m}_{liq} \tag{5}$$

In literature, [48], vapor mass flow rate is evaluated as the product of mass flow rate leaving the lamination valve (HPV) multiplied by the quality of working fluid ($q_{PS_{in}}$) entering the separator (Eq. (6)). Vapor quality is defined as the ratio between the vapor mass flow rate and that of the whole mixture. A slight deviation could be observed measuring the mass flow rate in vapor line $\dot{m}_{vap}$, this is due to the internal

Table 3
Measurement instrument and uncertainty.

Quantity	*Instrumentation*	*Uncertainty*
CO_2 temperatures	PT1000 RTD	±0.1 °C
Water/glycol temperatures	K-thermocouple	±1.5 °C
CO_2 flow rates	Coriolis flow meter	0.1 %
Water/glycol flow rates	Magnetic flow meter	0.25 %
CO_2 pressures	Membrane sensor	1 %

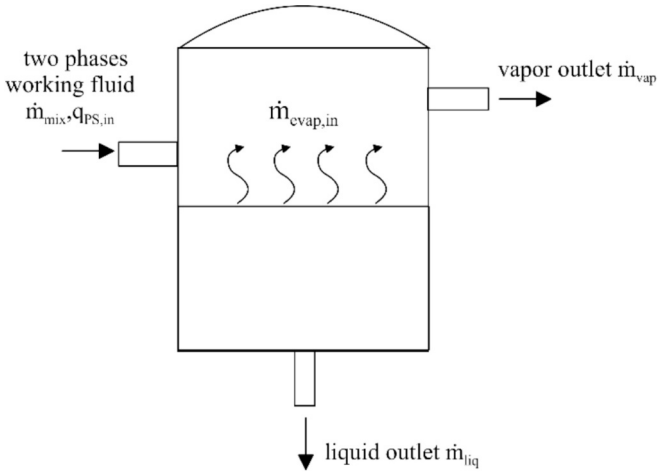

Fig. 5. 1-D Model scheme of phase separator tank.

evaporated current $\dot{m}_{evap,in}$. Hence, the internal evaporated mass flow rate can be evaluated by the difference of the vapor mass flow rate exiting the phase separator and the product of the mass flow rate entering the phase separator and the corresponding quality, [47].

$$\dot{m}_{evap,in} = \dot{m}_{vap} - \dot{m}_{CO_2} q_{PS_{in}} \tag{6}$$

In case of a proper thermal insulation the internal evaporated mass flow rate depends only on inner phenomena and not on ambient heat gain. It is worth to remark that an important parameter of phase separator is the height of the tank. This parameter, indeed, have a significant influence on the pressure at tank outlet due to the gravity effects.

Concerning the operating conditions, compressor speed are kept constant to 1450 RPM whereas the HPV valve was varied to maximize the compressor discharge pressure in every working conditions. The water flowing at evaporator presents a flow rate of 54 l/min and an inlet temperature varying from 22 °C up to 37 °C. The boundary conditions and the flow process of the model was resumed in Fig. 5.

It is important to notice that in the case of layout with expander (Fig. 2(a)), HPV is replaced by a SVRE. SVRE is modelled thanks to a 0D model (capacitive) based on the mass conservation equation, (Eq. (7)):

$$\dot{m}_{CO_2} = \frac{\rho_{int} V_{int} \omega_{exp}}{\eta_{exp}} \tag{7}$$

The opening of the intake and exhaust ports of the expander has been represented according to the real geometry as well as the filling and emptying of the vanes considered as small capacities which during filling loose the inlet kinetic energy of the refrigerating fluid while during discharging keep it, transforming it into a pressure decrease at the outlet section. When the fluid is inside the rotating vanes, the mass is conserved apart from the eventual leakages between adjacent vanes. The thermodynamic properties of the refrigerating fluid inside the vanes have been calculated according to the transformations which happen and with the equation of state for the liquid and for the vapor (and mixtures) evaluated with REFPROP: For sake of completeness, the expander model correctly reproduces all the other relevant aspect as blade motion, forces acting on them and on the stator surfaces, leakages between lateral blade and slot surfaces, cavitation phenomena in the fluid. Thanks to this approach, it has been possible to evaluate the expander permeability providing a fundamental relationship between the mass flow rate entering the expander and the mass flow rate crossing it (the one delivered by the compressor). Eq. (7) introduces intake volume, expander speed and volumetric efficiency whose values significantly affects the permeability. In particular, it can be remarked that the intake volume (which is one of the main outcomes of the design phase) presents a significant effect on the plant behavior considering that the expander behaves like a "revolving valve" with an intake volume which is passed, with a frequency given by the revolution speed multiplied by number of blades (vanes), from inlet to outlet. This immediately explains how important the expander design is (the intake volume, definitively) on the effect on the whole plant seen by the expander, represented by the overall refrigerating unit.

For each component of the model reported in Fig. 3, the input variables (Fig. 6) have been applied as boundary conditions:

a) At the "slave section" of the evaporator (cold side): mass flow rate, inlet temperature (i) and outlet pressure (l) of the water-glycol mixture;
b) At the "slave section" of the gas cooler (hot source): mass flow rate, inlet temperature (n) and outlet pressure (o) of the external air;
c) For the compressor (m): speed of rotation which defines the flow rate of the refrigerating fluid, the one circulating inside the system, according to the compressor pressure ratio;
d) At the High-Pressure valve (HPV), Flash gas valve (FGV) and EPV: the opening values which define the hydraulic impedance of the system;
e) When the expander (p) is considered: the speed of rotation. The presence of a regenerative inverter is considered to vary the expander speed such a way to control the expander permeability (Eq. 7).

Regarding the output variables, the model provides all the main operating variables of the refrigeration unit.

3. Results

3.1. Experimental results

To experimentally validate the model, the *trans*-critical CO_2 refrigeration unit was experimentally tested to assess its behaviour as function of the external temperature. The experimental data are collected for an entire summer day in July in the Centre of Italy. The acquisition lasts 24 h with an air temperature ranging from 18 °C up to 32 °C. Concerning the operating conditions, compressor speed are kept constant to 1450 RPM whereas the HPV valve was varied to maximize the discharge pressure. The raw data are post processed considering only the steady state operating conditions. The experimental data are then averaged and represented for each external temperature. During the experiments intermediate pressure are regulated acting on the High Pressure Valve (HPV) and Flash Gas Valve (FGV). The closing rate of HPV defines the pressure loss across the HPV and consequently the pressure upstream the separator tank (intermediate pressure). Moreover, it was observed that reducing the opening rate of the FGV, the pressure inside the tank tends to increase. The reduction of HPV opening rate affects also the maximum pressure as the permeability of the circuit decreases. In this occurrence pressure grows up to the achievement of *trans*-critical conditions.

The refrigeration unit performances have been tested during a summer period in the Centre of Italy with an air temperature ranging from 18 °C up to 32 °C.

As the aim of the analysis was to observe the effect of external air, the compressor operates at a fixed speed of 1450 RPM and the flow rate of the water-glycol mixture at evaporator and the air at gas cooler are respectively equal to 54 l/min and 7600 m^3/h.

As theoretical expected, external air presents a large impact on plant performance as it can be seen in Fig. 7 for the discharge pressure (Fig. 7 (a)) and temperature (Fig. 7(b)). Indeed, with the external air temperature which increases from 18 °C up to 32 °C, the pressure of the working fluid at the compressor outlet raises from 6.8 MPa up to 8.5 MPa (Fig. 8(a)). The raise of the discharge pressure leads to the increase of pressure ratio as the suction pressure remains quite constant when external air temperature varies (Fig. 8(c)). This explains the growth of discharge temperature with external air reported in Fig. 7(b). Regarding suction temperature, it exhibits a low increase with external air

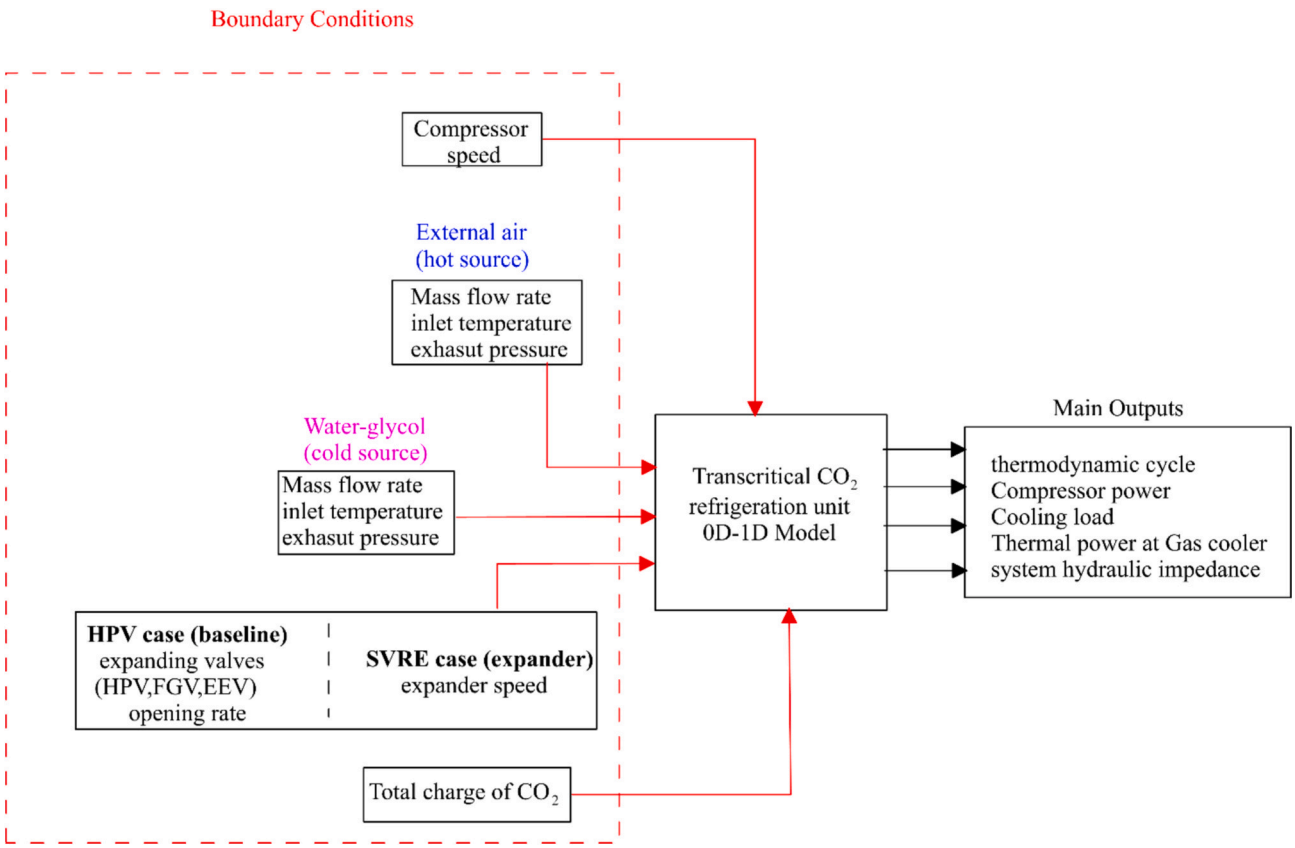

Fig. 6. Flow chart of the model.

temperature excursions. Hence, when the external temperature grows, an increase of plant maximum pressure (at compressor discharge) is observed. If the pressure exceeds the critical pressure, the refrigeration unit operates in *trans*-critical mode as it can be seen in Fig. 8 from the pressure-total enthalpy diagram reported for different air external temperature.

In Fig. 8 it can be seen the reference thermodynamic cycle to which the system refers (blue line) for external air temperature of 18 °C (Fig. 8 (a)), 24 °C (Fig. 8(b)), 27 °C (Fig. 8(c)) and 33 °C (Fig. 8(b)). For an external air temperature higher than 24 °C the discharge pressure exceeds the critical pressure, hence, below this value the unit operates in subcritical mode. Trans-critical and subcritical conditions influence the thermal power exchange between the refrigerating working fluid and the cold source. As matter of fact, in subcritical operation, the working fluid enters the gas cooler as superheated vapor exiting it as a subcooled liquid (Fig. 8 (a) and (b)). On the other hand, in *trans*-critical mode, the working fluid enters and leaves the gas cooler as a superheated vapor without a phase transition (Fig. 8(c) and (d)). It can be noticed as when the external air increases an enhancement of the of the quality of working fluid downstream HPV (Fig. 9) is reported. Indeed, in Fig. 9(a), the intermediate pressure (downstream HPV) is kept close to 35 bar (3.5 MPa) while the working fluid quality grows with external temperature (Fig. 9(b)). The quality increase explains as the working fluid towards evaporators decreases as the external temperature grows. Indeed, the higher the quality the lower the liquid is present in the separator tank and this leads to a decrease of the refrigerating working fluid towards the evaporator. When the quality is larger, the amount of refrigerating fluid mass flow rate forwarded to the flash gas valve increases. This mass flow rate is due to the difference between the total mass flow rate provided by compressor (Fig. 9(c)) and that provided to the evaporator (Fig. 9(d)).

In Fig. 10 the compressor power (a), cooling load (b), COP of the refrigerating unit (c) were reported. When the external air temperature grows, compressor power raises from 4 kW up to 5 kW due to the increase of discharge pressure, and consequently, to the increase of compression ratio, Fig. 7(a). The cooling load (the thermal power extracted from evaporators) exhibits a decrease due to the reduction of the refrigerating mass flow rate forwarded to the evaporator when the external air grows. The trend of these quantities explains as the COP diminishes from 3.5 up to 2 due to the combined effects of compressor power decrease and cooling load decrease. For sake of completeness, COP is defined as the ratio between the extracted thermal power (cooling load) and compressor power as in (Eq. (8)):

$$COP = \frac{P_{th,Evaps}}{P_{compr}} \tag{8}$$

3.2. Model validation

A further novelty of the work is the analysis of the expander impact on plant behaviour through a comprehensive model of the whole unit. To do this is fundamental that the model can reproduce in accurate way all the main parameters of the system. Indeed, the aim of the novel expander design approach is that expander does not produce a significant variation of the original parameters of the baseline case. Hence, to demonstrate the reliability and accuracy of the model, the low errors between experiments and predictions was reported.

The Absolute and Relative Root Mean Square Error (Eqs. (9) and (10)) and Maximum Absolute and Relative Deviation (Eqs. (11) and (12)) are chosen to assess the accuracy of the model with the predicted values.

$$RMSE = \sqrt{\frac{\sum_{i=1}^{N}\left(x_i - \check{x}_i\right)^2}{N}} \tag{9}$$

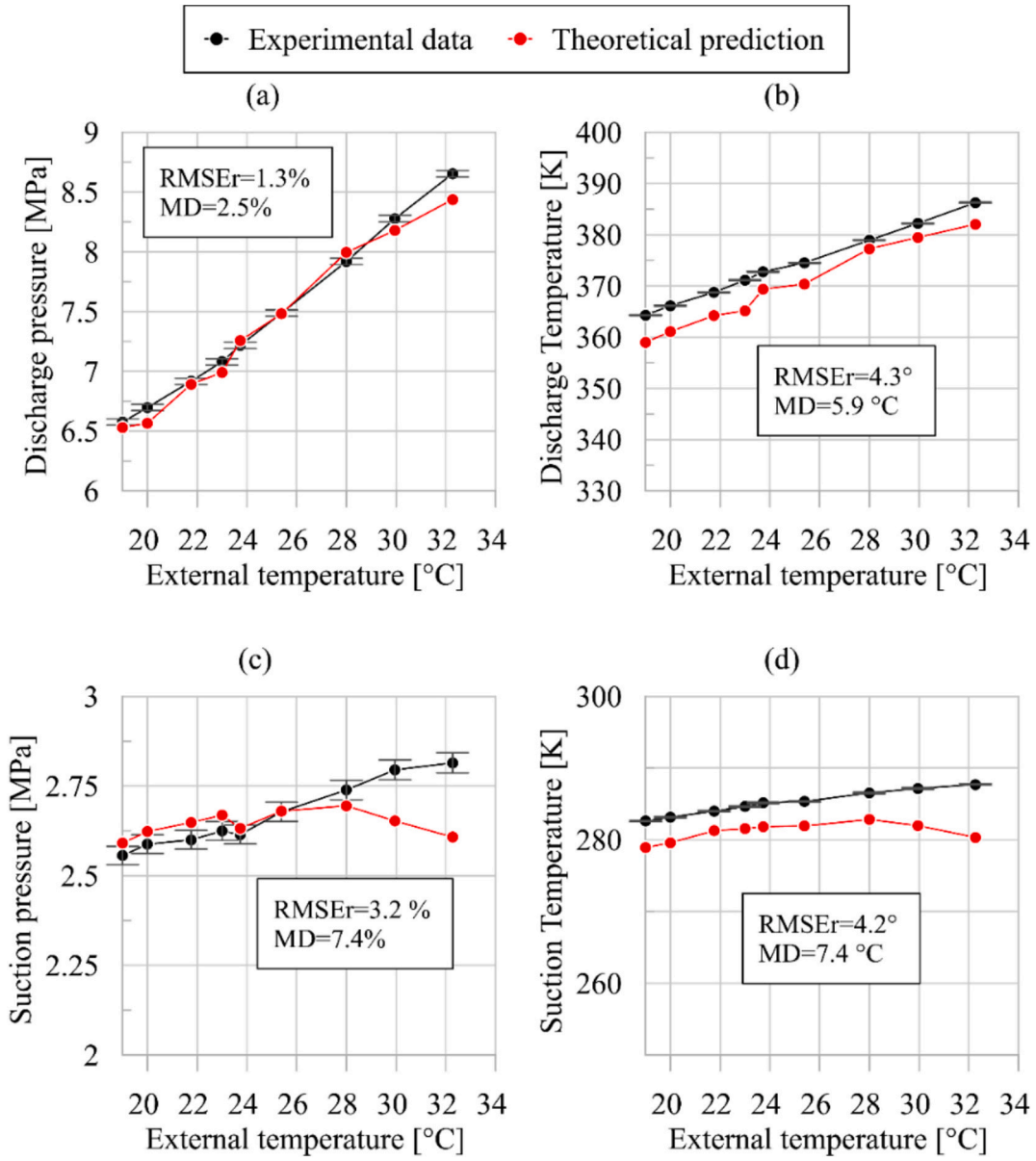

Fig. 7. Experimental and theoretical discharge pressure (a) and temperature (b) and suction pressure (c) and temperature (d) of working fluid as function of external temperature. Experimental errors bar are reported as vertical squared lines.

$$RMSEr = \sqrt{\frac{\sum_{i=1}^{N}\left(\frac{x_i - \check{x}_i}{\check{x}_i}\right)^2}{N}} \tag{10}$$

$$MD = max\left(\frac{x_i - \check{x}_i}{\check{x}_i}\right) \tag{11}$$

$$MD_r = max\left(x_i - \check{x}_i\right) \tag{12}$$

Concerning the predicted values given by the model, the following consideration apply.

Concerning discharge pressure, the agreement between experimental and theoretical data is really satisfying demonstrated by a low $RMSE_r$ and MD_r equal to 1.3 % and 2.5 %, respectively. The errors in terms of discharge temperature are slightly larger despite it can be retained fully satisfying being the RMSE and MD of 4.3 °C and 5.9 °C, respectively. This is due to the unavoidable simplifications and assumptions of the evaporator geometry to obtain a 1D model. The authors expect for previous similar calculations that in presence of a geometrical data of this component more detailed, the temperature difference could be below 1.5 °C. A high accuracy is reached for the suction pressure values, with a $RMSE_r$ and MD_r respectively equals to 3.2 % and 7.4 %. Concerning the suction temperature, the same consideration made for discharge temperature applies. The good accuracy is good with a RMSE = 4.2 °C and a MD = 4.2 °C and 7.4 °C. The good agreement between experimental data and predictions can be seen in Fig. 7.

Concerning the intermediate pressure (downstream the HPV valve) the RMSEr is 1.9 % whereas the MDr is 3.6 %. An interesting aspect is the good agreement between experimental refrigerating fluid quality at HPV and the prediction. Indeed, in Fig. 9 the model follows the experimental trend, with a low RMSEr (6 %). The consequence of this good prediction is a similar good representation of the refrigerating fluid mass flow rate provided by the compressor and that forwarded to the evaporator. For these quantities, a RMSEr of 4.4 % and 4.6 % are observed, respectively.

A final consequence of the satisfying predictions of the model is the

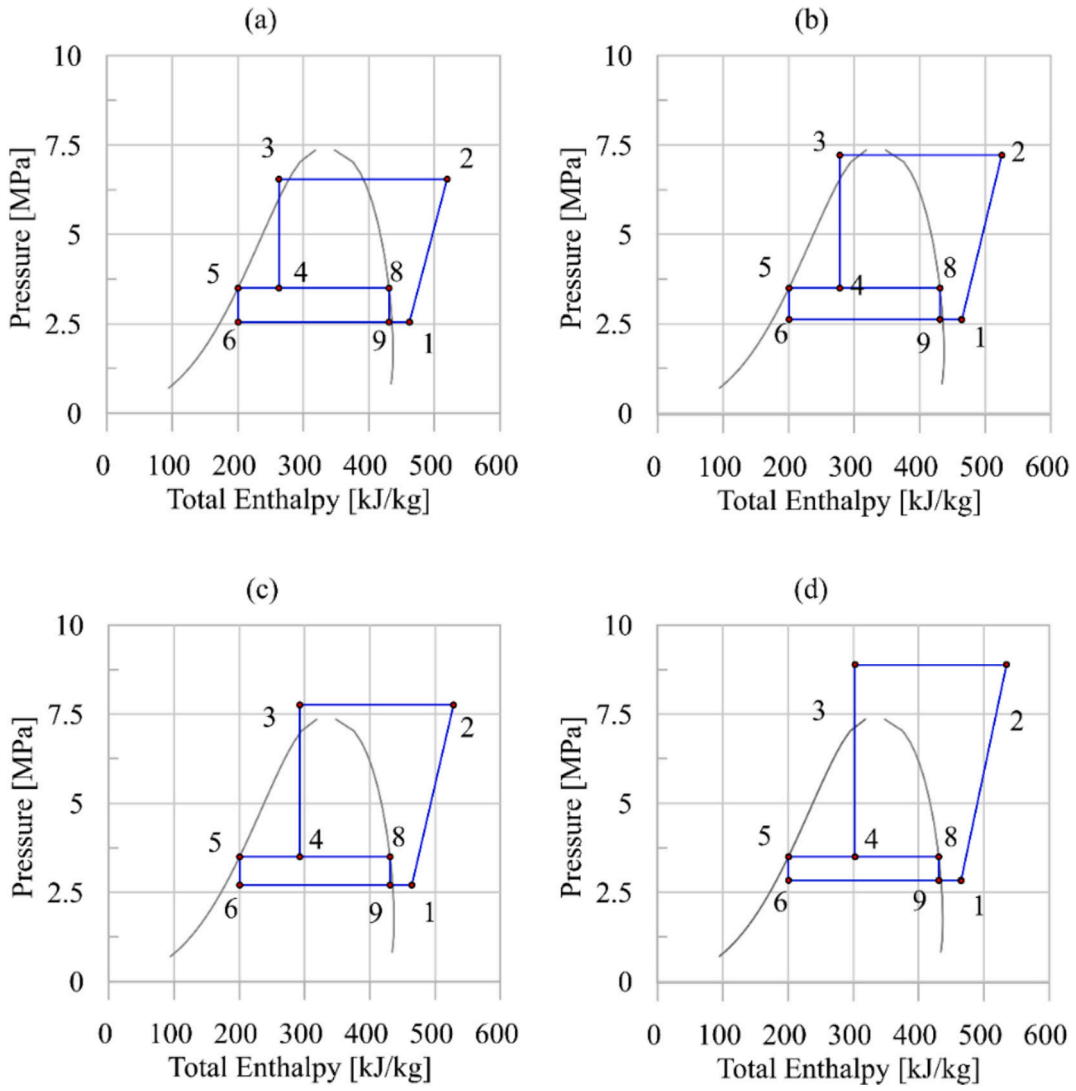

Fig. 8. Pressure-Total Enthalpy diagram for external temperature equals to 18 °C (a), 24 °C (b), 27 °C (c) and 33 °C (d).

capability to represent with high accuracy the power required by compressor which changes from 4 kW up to 5.5 kW (Fig. 10). In this case the RMSEr and the MDr are 3 % and 5.7 %, respectively. The thermal power extracted by evaporators has a $RMSEr_{\%}$ equal to 8.2 % while the COP (Eq. (4)) a $RMSE_{\%}$ of 8.5 %. The p-h diagram reported in Fig. 10(d) demonstrates a complete very satisfactory overlapping between predictions and tests.

3.3. Assessment of the separator volume size on plant performance

Once validated, the model can be used to investigate some plant features which cannot be analysed with a thermodynamic model. For instance, the impact of tank separator on the whole plant behaviour can be assessed only with a capacitive model as the one developed in this works. Indeed, this component is placed downstream the HPV valve and it ensures to separate the liquid from vapor phase. The choice on this components was due to the lack of references in literature to design this component whose cost and steel consumption are significant. This could be helpful also in light of the expander design as according to the tank volume selection the pressure downstream expander could change, thus affecting its expansion ratio. Liquid phase then flows towards evaporators while vapor is forwarded to flash gas valve. Hence, thanks to the model, the impact of volume size of separator tank on the whole plant behaviour was observed for a CO_2 charging mass of 15 kg and an external temperature of 33 °C. In Fig. 11 (a) and (b) decreasing the Separator Volume from 160 up to 30 L the maximum plant pressure grows from 6 up to 25 MPa. A same trend is observed for also for temperature which grows from 380 up to 430 K. Also, the pressure downstream the HPV valve (Fig. 12(a)) sees a similar increase from 3 MPa up to 5.5 MPa with Volume reduction from 160 up to 30 L. This means that when separator volume diminishes an increase of all pressure levels of the unit takes place. Hence, also the pressure inside the tank grows which is equal to that downstream of HPV (Fig. 12(a)). This leads to a larger amount of liquid mass inside the separator which passes from 3 % up to 15 % (Fig. 13(a)) when the volume is reduced from 160 up to 30 L. This involves a larger working fluid mass flow rate (Fig. 12(b)) and, simultaneously, a larger portion forwarded to the evaporators being lower the quality of CO_2 downstream the HPV for lower volume (Fig. 13 (b)). Quality is, indeed, expressed as the volume fraction of vapor on all the mixture (Fig. 14(a)).

The separator tank was modelled as a lumped volume. It was seen as the ratio between the mass charge of the working fluid define the base pressure of the unit. A larger volume of the separator contributes to increase the whole plant volume equal to 0.12 m^3 for the case at hand. So, for a given charge of working fluid (15 kg for the case at hand), the ratio between the mass charge and the plant volume decreases thus providing a reduction of the minimum plant pressure.

Consequently, the thermal power extracted (Cooling load) increases

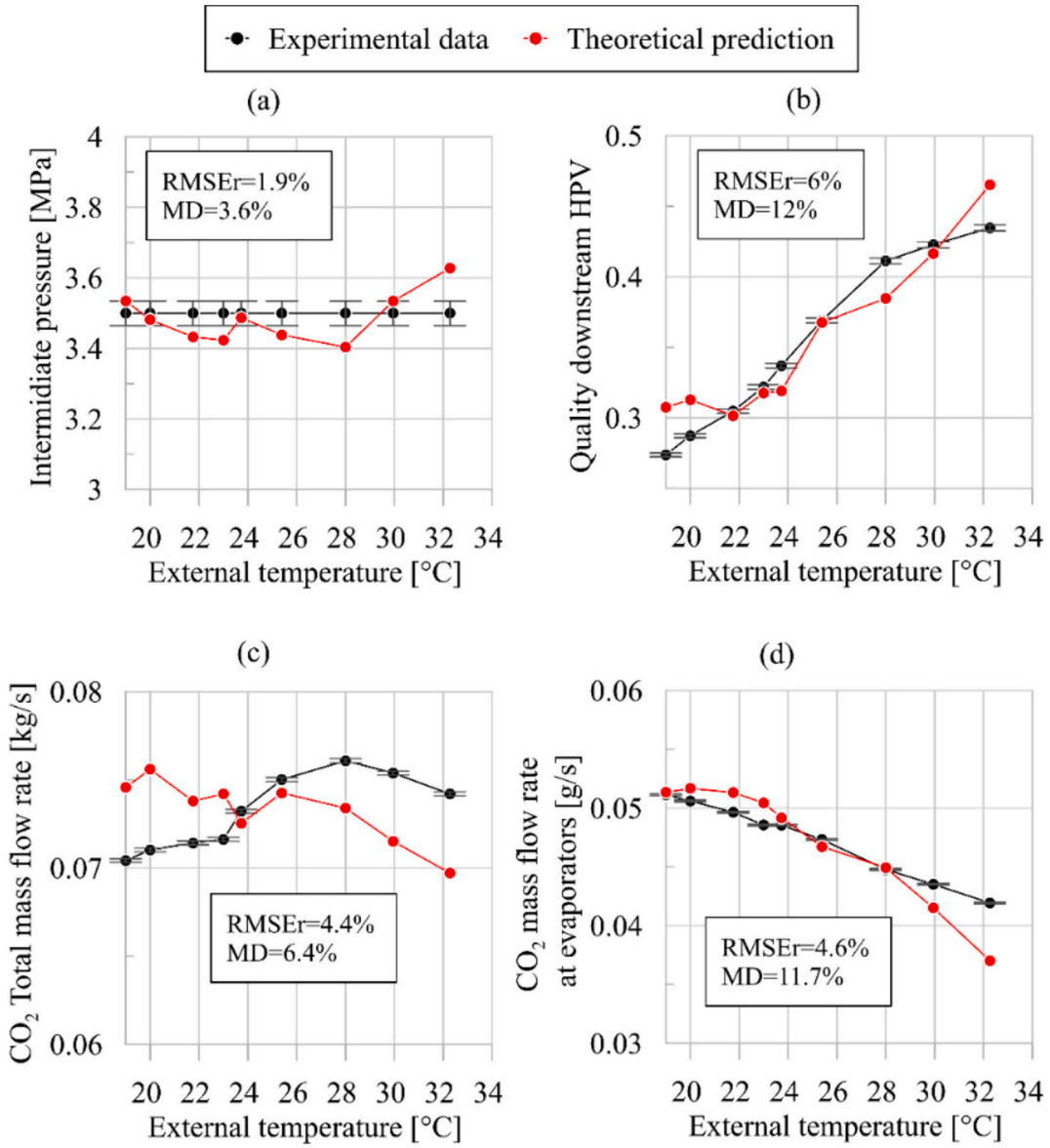

Fig. 9. Experimental and theoretical intermediate pressure (a) and quality of working fluid at HPV outlet (b) and CO_2 total mass flow rate (c) and at evaporator (d) as function of external temperature. Experimental errors bars are reported as vertical squared lines.

from 3 kW up to 30 kW when volume of the tank decreases from 160 L up to 30 L (Fig. 14(b)). Hence, the decrease of Volume of the separator leads to a higher cooling load but involves a larger pressure levels and working fluids to elaborate. This causes the increases of power required by compressor which sees a significant grows from 3 up to 15 kW when volume of the separator passes from 160 L up to 30 L. Consequently, COP assumes a maximum close to 2.8 for a volume equal to 80 L (Fig. 15(b)). Indeed, COP decreases for too low and too high volume because in the first case the compressor power is larger (Fig. 15(a)) while in the second case a too low cooling load is observed (Fig. 14(b)). Therefore, a general recommendation for the design is to select an intermediate value for the separator tank to ensure a proper cooling load avoiding that compressor power reaches unsuitable value. It is important to observe that the volume of the tank of the experimented unit is 110 L and reducing this value to 80 L an increase of 12 % can be achieved on COP.

The achieved results are in accordance with literature according to which the adoption of a larger receivers ensures to increases the range of refrigerant charge according to which optimal conditions are reached, [49].

3.4. Sliding rotary vane expander design

Once validated, the model of the unit was used to refine the expander design of the intake volume which was preliminary designed thanks to a theoretical approach based on mass conservation between the working fluid exiting the gas cooler and that elaborated by the expander (Eq. (5)).

The main outcome of this preliminary design is the intake volume, considering as an input the expander speed (1500 RPM) and the volumetric efficiency taken from literature for this kind of device [31,32] and taken equal to 60 %.

Considering as rated point the one corresponding to the average summer temperature 25.4 °C, the following operating quantities are considered:

- Temperature of CO_2 at expander inlet equal to 29 °C;
- Pressure of CO_2 at expander inlet equal to 74.2 bar (7.42 MPa);
- Pressure of CO_2 downstream the expander of 35 bar (3.5 MPa);
- CO_2 working fluid mass flow rate entering the expander equal to 75 g/s.

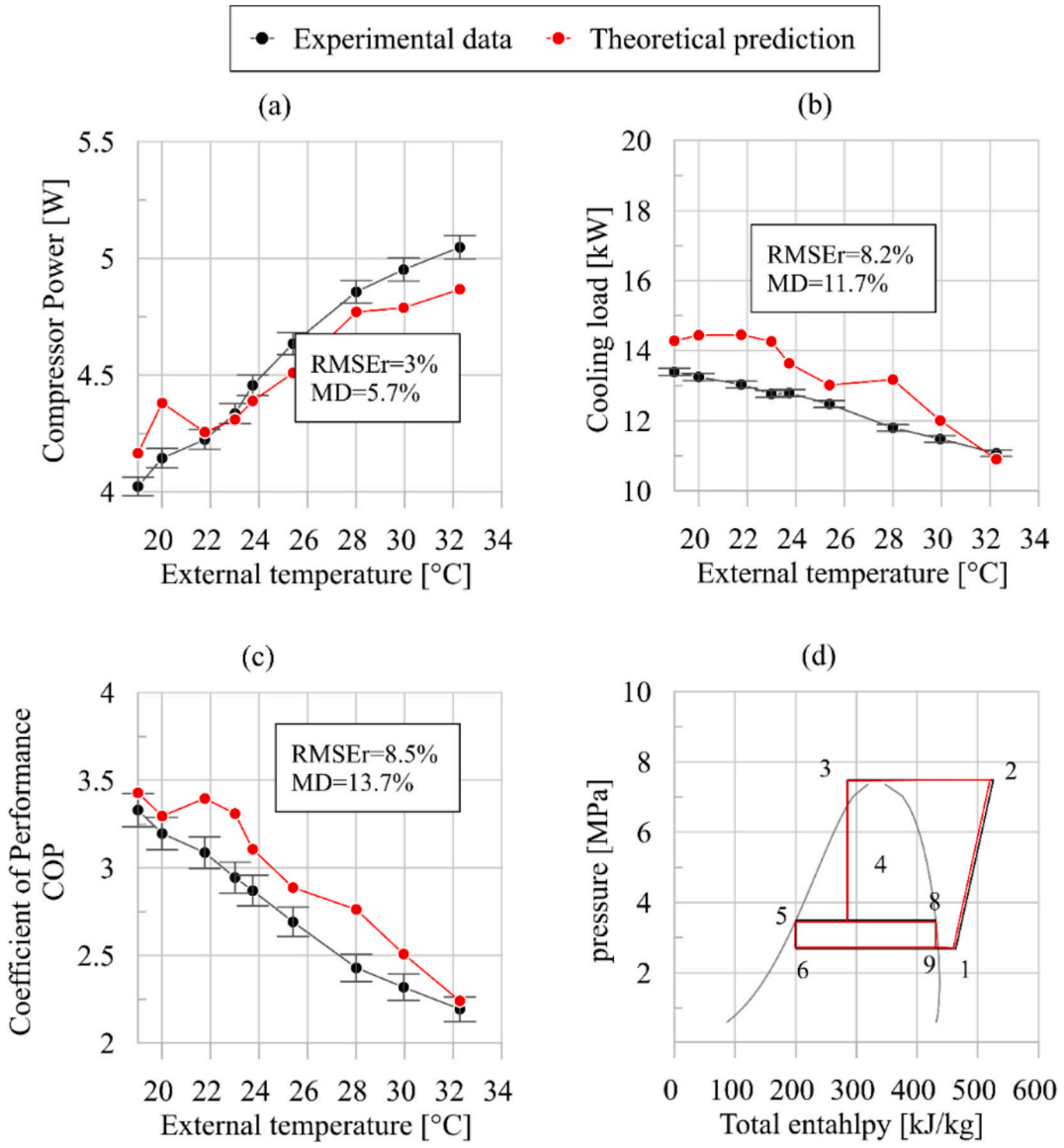

Fig. 10. Experimental and theoretical compressor power (a), cooling load (b) and COP (c) as function of external temperature. Experimental errors bar are reported as vertical squared lines.; experimental and theoretical pressure-total enthalpy p-h diagram for an external temperature of 25.4 °C.

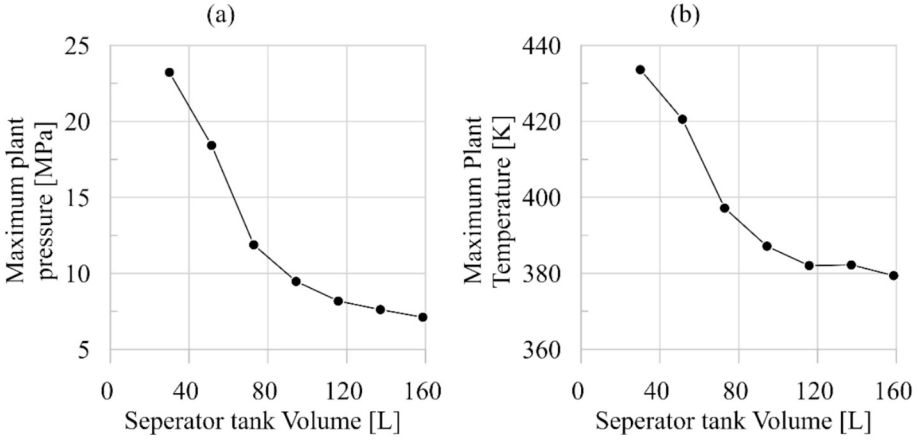

Fig. 11. Maximum plant pressure (a) and temperature (b) as function of separator volume.

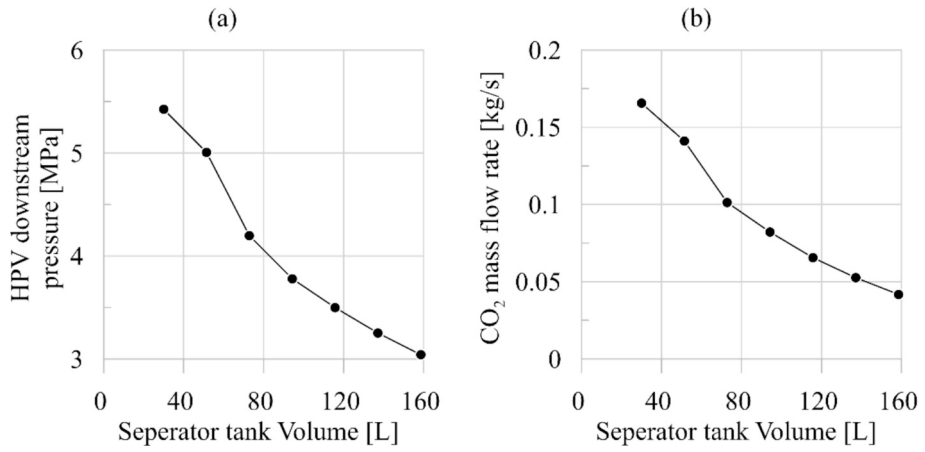

Fig. 12. HPV downstream pressure (a) and CO_2 mass flow rate (b) as function of separator volume.

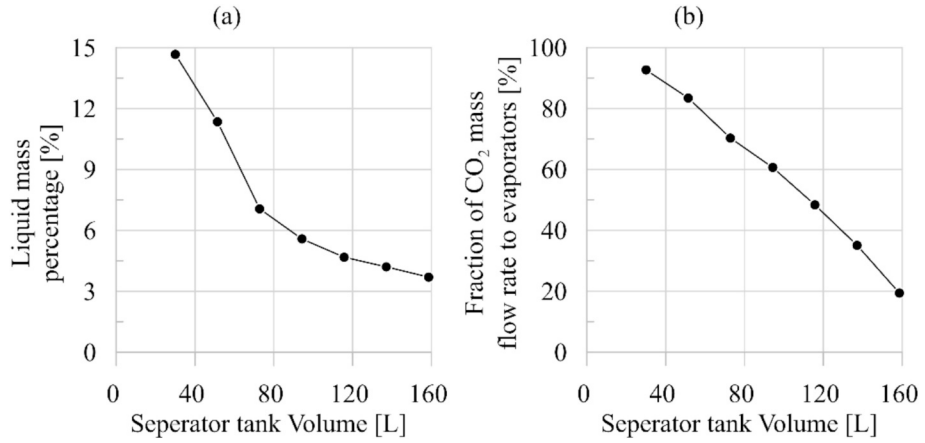

Fig. 13. Liquid phase mass percentage inside separator (a) and fraction of CO_2 mass flow rate (b) forwarded to evaporators as function of separator volume.

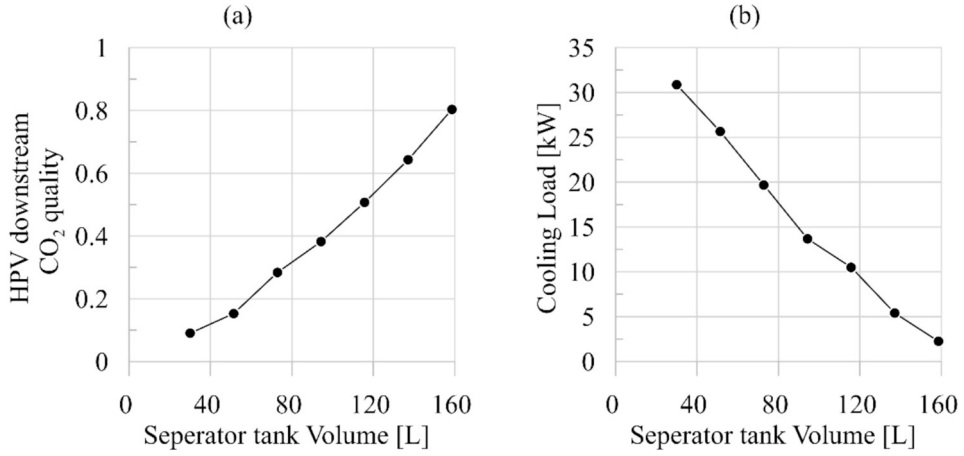

Fig. 14. CO_2 quality downstream HPV (a) and fraction of CO_2 mass flow rate (b) forwarded to evaporators as function of separator volume.

According to these parameters, the preliminary expander intake volume coming from Eq. (3) is equal to 2.63 cm^3.

Assuming this datum, the speed that the expander must assume when the operating conditions varies was evaluated reversing Eq. (3). Indeed, imposing the preliminary intake volume (2.63 cm^3), expander speed can be known as operating conditions (and consequently density of the CO_2 at expander intake change). Hence, with an intake volume of V_{int} equal to 2.63 cm^3 expander speed should varies between 1200 RPM and 1600 RPM as in Fig. 16(a), according to the external temperature which varies from 18 °C to 32 °C. In all the operating point expander receives at inlet a working fluid in subcooled or a supercritical working conditions.

Observing the expander intake pressure (black line) given by the model (Fig. 16(b), baseline), it can be seen that the preliminary expander design having 2.63 cm^3 as intake volume requires a slight variation in order to better match the reference datum. This happens if a V_{int} is reduced to 2.5 cm^3.

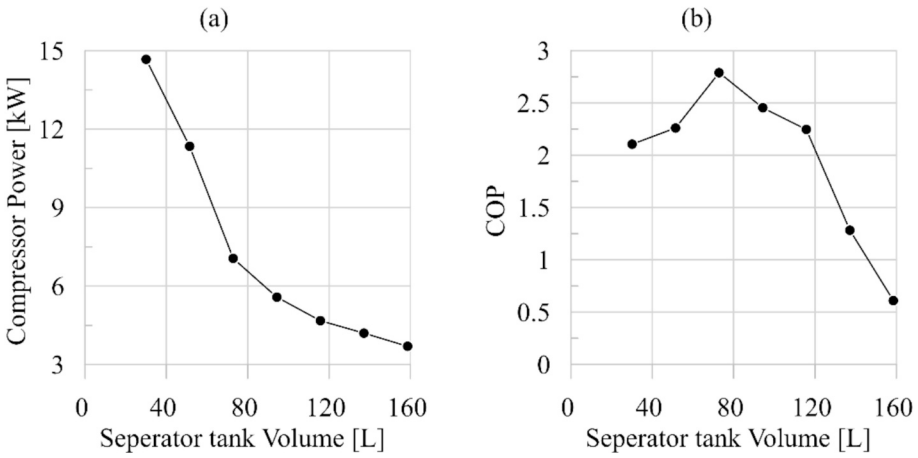

Fig. 15. Compressor Power (a) and COP (b) as function of separator volume.

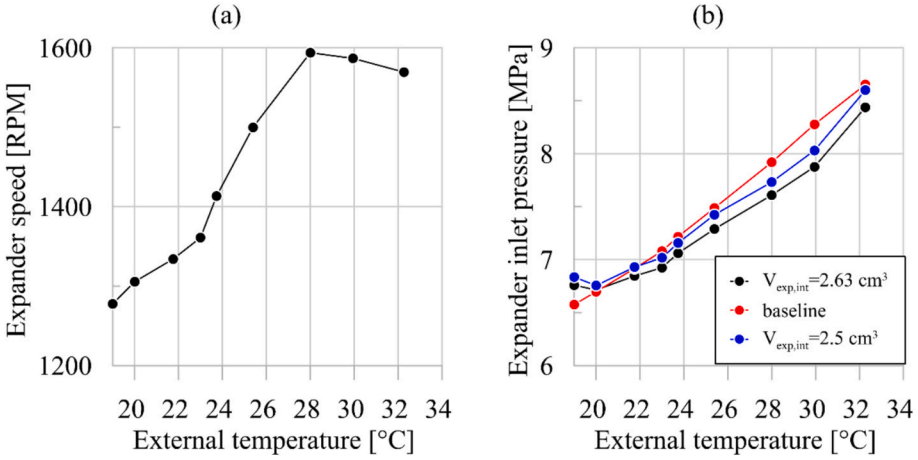

Fig. 16. Expander speed (a) and expander inlet pressure in baseline and SVRE case with an intake volume of 2.63 cm^3 and 2.5 cm^3.

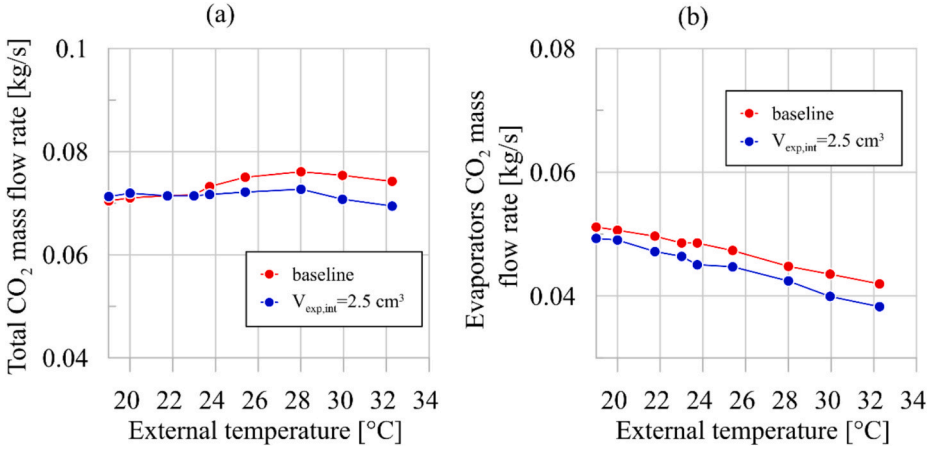

Fig. 17. Total (a) and evaporator (b) CO_2 mass flow rate in baseline and SVRE case.

Assuming this new value, Fig. 17 (a) and Fig. 17 (b) show how close are the two predictions on the refrigerating fluid mass flow rate (a) and on that at the evaporators (b), between the baseline case (HPV presence, baseline case) and when the expander (having a V_{int} = 2,5 cm^3) substitutes the HPV. This definitively ensures that the substitution of the HPV with the SVRE, suitably controlled in RPM, does not produce a significant variation of the fluid dynamical and thermodynamical properties of the refrigerating unit.

It is worth to remark that when expander was considered, to keep the same operating conditions of the HPV case, the speed was varied in order to set its permeability (i.e. attitude to be crossed by working fluid). Permeability defines the plant maximum pressure for a given mass flowrate entering the expander. Hence, observing Fig. 16, the total mass flow rate (entering the expander) tends to increase in the range 24–28 °C

and decrease from 28 °C up to 32 °C. The expander speed increases in the temperature range of 24–28 °C to increase the permeability to avoid that maximum pressures see a too high increase. On the contrary, between 28 °C and 32 °C the expander speed diminishes to reduce plant permeability and avoid that pressure assumes too low values. Definitively, the expander speed which can be changed very easily represents a suitable control variable to restore the previous cooling capacity of the unit (with its thermodynamic performances), while the power recovered by the expander remains the useful effect in terms of COP increase. Hence, expander intake pressure represents the value at the outlet of dry cooler and the inlet of the HPV. In the present paper the operating condition of the expander was set in order to keep the same value of baseline case (with HPV).

Once the expander intake volume was defined, the SVRE could be built (keeping the same intake volume) with two shape configurations. A finger-shapes configuration can be achieved with a predominant axial dimension whereas a disk-shaped one by a radial development. To orient the design the comprehensive expander model experimentally validated by authors in previous works [42,43] has been used. It produced a design with the main dimensional characteristics reported in Fig. 18. The θ angle is evaluated by the bisector line (dashed line) of chamber 1 and reference line. Eight blades were considered as best compromise between the optimization of mechanical and volumetric efficiency. Indeed, increasing the blade number the volumetric losses tend to decrease as the angular interval of pressure difference between adjacent vane is lower, [50]. Anyway, if the blade number increases, this provides a growth of mechanical friction losses.

3.5. The dual intake port expander

Dual Intake Port (DIP) technology involves the introduction of a second intake port after the mean one, ensuring that machine can be continuously filled even during vane expansion, [42,43]. Thanks to this approach, two main benefits were observed:

1. The machine can elaborate a larger amount of fluid for a given pressure difference at its sides.
2. The pressure decrease during the expansion phase is delayed leading to a larger area in the P-V plane. This means that the work produced by the expander is greater.

Thanks to the afore mentioned pressure decrease, some additional benefits also on volumetric efficiency are introduced. The main leakages path was considered the volumetric losses between the blade tip and the stator inner surface, the one between blade side and rotor slot and that between rotor face and machine casing. Moreover, also the leakages across the tangency were considered. Among the leakages path the one which affects most the volumetric losses is the leakages between blade tip and stator inner surface, [50].

DIP delays the end of intake phase, so, the interval angle in correspondence to which the pressure difference between adjacent chambers takes places diminishes and leakages are reduced.

In Fig. 19 the scheme of DIP SVRE was shown as a result of the procedure in [42,43] while in Fig. 18 the conventional solution is reported (Single Intake Port, SIP). The angular configuration of second inlet was chosen to achieve the best compromise between power production increase and machine efficiency. Indeed, according to the experimental and theoretical analysis carried out by the author in [42,43] it was seen that the power production tends to increase for dual intake port angle far from the main one (avoiding of course any overlap with the exhaust port). On the other hand, the efficiency tends to increase reducing the distance of the intake ports. So, the proposed solution allows to solve the trade-off problem.

In Fig. 20(a), SIP and DIP expanders are fed by the same inlet pressure (the curves are overlapped) and the exhaust pressure is equal to 3.5 MPa. DIP solution elaborates a larger mass flow rate than SIP (Fig. 20 (b)). This is the effect of the machine permeability increases.

The extra flow rate of the refrigerating fluid ensures that DIP expander produces a higher power (Fig. 21(a)). A benefit in volumetric efficiency is also observed from Fig. 21(b) −from 0.6 up to 0.72- as already observed from expected theoretical considerations. The higher volumetric capacity of DIP expander is demonstrated by the PV diagram (Fig. 22). DIP machine presents a larger intake section (up to 0.61 cm^3) than the SIP one. This delays the pressure decrease, resulting the vane of the DIP expander filled even during the first part of the expansion phase (increase of the vane volume). This allows to produce two benefits. The first is that increasing the intake phase, the pressure difference between a chamber and the preceding and following ones is limited to the last portion of expansion.

Fig. 22 reports a theoretical prediction of pressure trace inside chambers. This prediction can be retained more accurate as the model was validated against experimental data related to measurement of pressure inside the vane. In authors work [43] the measurement process is reported, it can be seen that three piezoresistive pressure transducers was adopted with a frequency sampling of 4500 Hz. The sensors are placed in angular section allowing to reproduce the main phase of the intake, expansion and exhaust process. The measurement are evaluated as function of time, a post processing algorithm was developed which ensures to correlate the pressure to the angular position and subsequently, exploiting the geometrical relation linking the angle and chamber volume, the pV diagram can be outlined.

DIP machine presents a larger intake section (up to 0.61 cm^3) than the SIP one. This delays the pressure decrease, resulting the vane of the DIP expander filled even during the first part of the expansion phase (increase of the vane volume). This allows to produce two benefits. The first is that increasing the intake phase, the pressure difference between a chamber and the preceding and following ones is limited to the last portion of expansion (DIP case in Fig. 22). This allows to reduce the leakages losses according to what observed in [42]. The increase of volumetric efficiency positively impacts on mechanical efficiency which

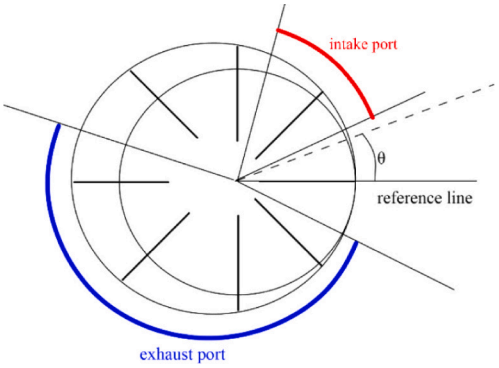

Rotor Diameter	34.9 mm
Stator Diameter	38 mm
Eccentricity	1.27 mm
Number of blades	8
Expander height	42 mm
Blade thickness	4 mm
Blade length	5 mm
Blade weight	3.9 g
Intake port opening angle	0 deg
Intake port closing angle	75 deg
Exhaust port opening angle	154 deg
Exhaust port closing angle	356 deg

Fig. 18. SVRE design.

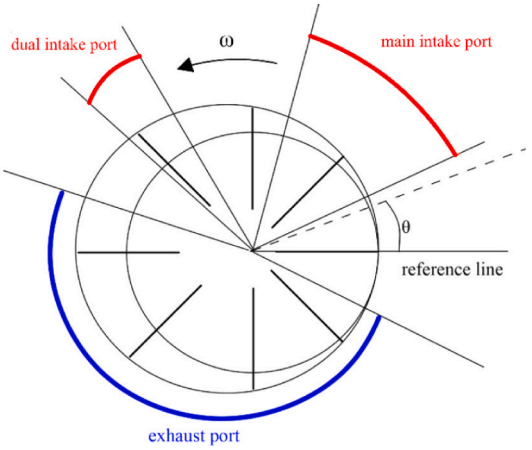

Rotor Diameter	34.9 mm
Stator Diameter	38 mm
Eccentricity	1.27 mm
Number of blades	8
Expander height	42 mm
Blade thickness	4 mm
Blade length	5 mm
Blade weight	3.9 g
Intake port opening angle	0 deg
Intake port closing angle	75 deg
Intake port opening angle	68 deg
Intake port closing angle	130 deg
Exhaust port opening angle	154 deg
Exhaust port closing angle	356 deg

Fig. 19. Dual Intake Port (DIP) SVRE design.

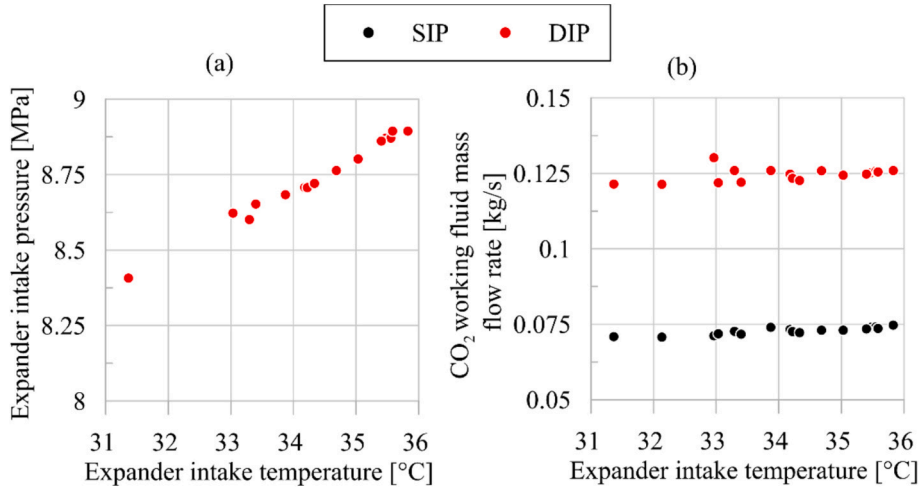

Fig. 20. Expander Intake pressure (a) and CO_2 mass flow rate (b) in SIP and DIP case as function of expander intake temperature.

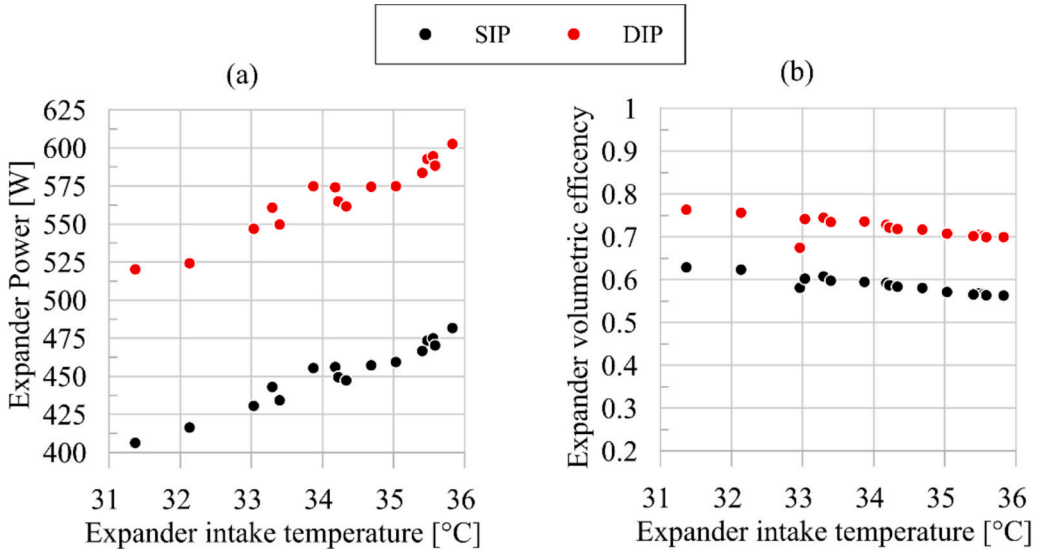

Fig. 21. Expander Power (a) and volumetric efficiency (b) in SIP and DIP case as function of expander intake temperature.

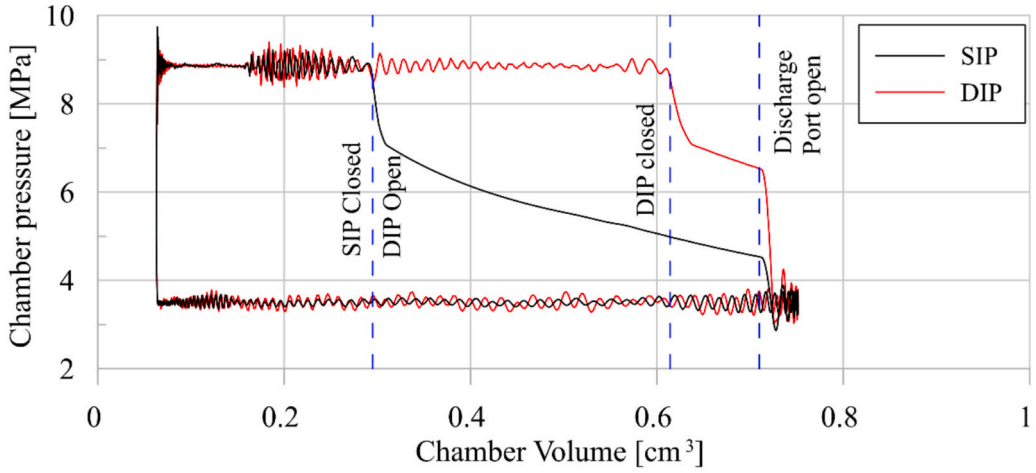

Fig. 22. Comparison between chamber pressure vs chamber volume (indicated cycle) in SIP and DIP case.

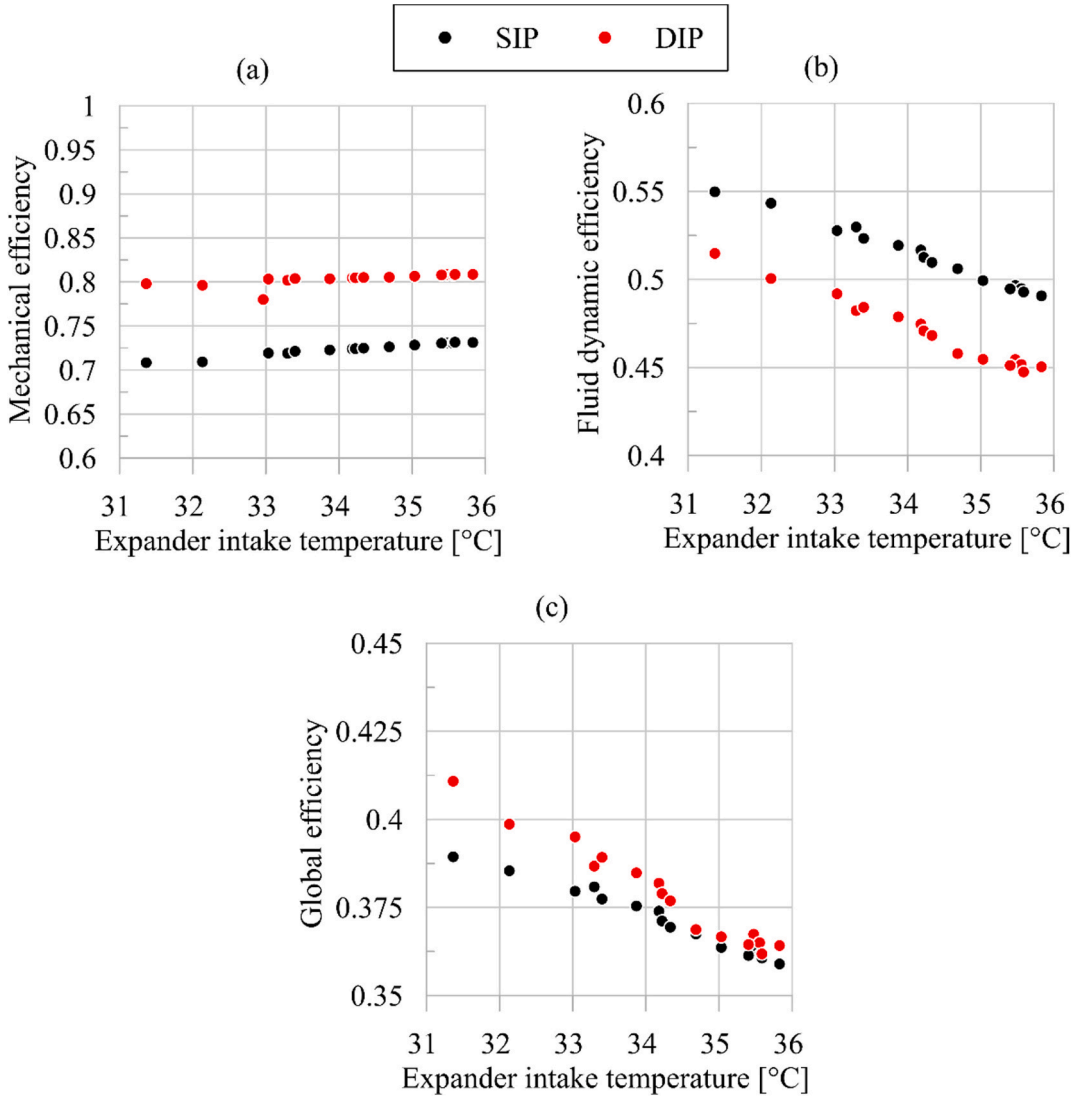

Fig. 23. Mechanical (a) Fluid dynamic (b) and global efficiency (c) in SIP and DIP case.

grows thanks to the adoption of DIP as it can be seen from Fig. 23(a).

Indeed, mechanical efficiency is evaluated as the ratio of mechanical power on the shaft and the indicated power (Eq. (13)) given by the area of indicated cycle in Fig. 22 evaluated as in Eq. (14):

$$\eta_{mech} = \frac{P_{mech}}{P_{ind}} \tag{13}$$

$$P_{ind} = \sum_{i=1}^{N_v} \frac{\oint p_i dV_i}{t_{cycle}} \tag{14}$$

where p_i is the pressure inside the i-chamber, V_i is the chamber volume, t_{cycle} is the time needed to complete a cycle and N_v is the number of chamber

As Fig. 22 shows, DIP allows to boost the indicated cycle and consequently its area. For this reason, DIP indicated power (exchanged between working fluid and mobile components) is larger than SIP. As the DIP does not provide a variation of machine dimensions, the friction power losses are the same and for Eq. (15) DIP mechanical power is larger than SIP.

$$P_{mech} = P_{ind} - P_{mech,loss} \tag{15}$$

Mechanical power represents the power on the expander shaft whereas the indicated one is the work exchanged by the working fluid and the machine mobile components. This means that the difference represents the friction losses.

Another positive aspect of DIP is that the typical sudden pressure loss encountered at the end of intake phase, already observed by [30] for SVRE operating with *trans*-critical CO_2, is delayed from 0.3 cm^3 (SIP case) up to 0.6 cm^3 (DIP case) hence DIP expander presents a larger pressure for a wider volume variation with respect SIP with a consequent benefit on indicated power. The delay of the intake phase produced by the introduction of DIP leads to a lower volume interval (from 0.61 cm^3 up to 0.75 cm^3) in which SVRE performs a closed volume expansion phase. Consequently, at the discharge port opening, the pressure inside DIP is larger than the corresponding value in SIP case. Thus, the power related to isochoric expansion is greater for DIP. Despite isochoric expansion collaborate to power production, the fluid dynamic efficiency (Fig. 23(b)) diminishes if an adiabatic isentropic expansion is taken as reference transformation (Eqn 16).

$$\eta_{fluid} = \frac{P_{ind}}{P_{ad,is}} = \frac{P_{ind}}{\dot{m}_{CO_2}\left(h_{in} - h_{out,is}\right)} \tag{16}$$

Indeed, adiabatic isentropic efficiency (global efficiency) (Fig. 23(c)) does not consider the isochoric expansion thus outlining a reduction of efficiency when the under-expansion is larger as in DIP case. So, a reference transformation more adherent to real behaviour of volumetric expander than adiabatic isentropic is needed. Anyway, as adiabatic isentropic efficiency is generally considered to express the whole expander behaviour it is employed also in this research. Eq. (17), can be rearranged to express the efficiency chain, [51]:

$$\eta_{exp} = \frac{P_{mech}}{P_{ad,is}} = \frac{P_{mech}}{P_{ind}} \frac{P_{ind}}{P_{ad,is}} = \eta_{mech}\eta_{fluid} \tag{17}$$

The expander whole efficiency depends by the product of the mechanical and fluid dynamic efficiency. The former considers the effect of friction losses the latter the detrimental effect of volumetric losses and deviation from ideal reference transformation. Besides the over and under expansion (when the pressure inside the chamber is lower or higher the one exerted by the circuit at expander outlet, respectively), fluid dynamic efficiency takes also into account the effect of volumetric efficiency which affect the working fluid entering the expander and consequently the indicated power.

It is interesting to observe that despite the lower fluid dynamic efficiency, the DIP presents a larger whole efficiency due to the larger mechanical efficiency. This confirms that DIP solution is not a simple supercharging technique, but it leads to a more performant machine with a larger power production and efficiency.

Authors widely experimentally analyse in previous work SIP and DIP also considering the effect of lubrication oil, 5 % in mass of the whole working fluid charge. Thanks to this wide database, theoretical model was validated and used as reliable and accurate software platform to optimize the expander design. For what regard lubrication, despite the model can predict its impact, for the application at hand an oil free expander was considered in order to avoid oil separator or an oil mixed to CO_2. Concerning the impact of this choice on volumetric efficiency, the adoption of DIP allows to overcome the absence of oil as it allows to reduce the leakages losses. For what concern the mechanical efficiency, an accurate design of the blade allowing to reduce as much as possible the contact area could be helpful to keep low the friction losses.

3.6. Assessment of benefits introduced by DIP expander in CO_2 trans-critical refrigeration unit with respect to a SIP expander and with respect to the original HPV

DIP introduction allows to improve the expander performance but also to increase its permeability. Hence, when introduced inside the CO_2 refrigeration unit (replacing a HPV) it is expected that, keeping constant the maximum plant pressure, the compressor can deliver more mass flow rate.

Indeed, it is useful to remark that a volumetric expander behaves like a “revolving valve”, hence, the larger is its permeability the lower is the hydraulic resistance that compressor sees. To observe the benefits introduced by a SVRE which replaces a HPV and a further improvement when a DIP technology is considered, the model of the whole unit modified in order to account for the mentioned plant modifications was used.

The comparison was carried out set DIP and SIP expander speed in order keep the same intake pressure at the HPV (Fig. 24(a)) and CO_2 mass flow rate (Fig. 24(b)). This guarantees that the conditions upstream the HPV were kept the same. The expander speed can be controlled with a regenerative inverter which allows to externally set the rated speed even if the electric generator is connected to the electric grid.

As a result of the increased permeability of the DIP technology, in Fig. 24(c) can be observed that in this case the expander speed is significantly lower due to the larger intake volume and volumetric efficiency increase (Fig. 21(b)). So, adopting a DIP expander, its speed of revolution can be significantly reduced (40 %). Consequently, benefits on friction loss reduction without penalties on volumetric capability and expected wear reduction too, i.e. longer operating life.

A further benefit of DIP is that with respect to SIP ensures to achieve a fraction of CO_2 mass flow rate forwarded to evaporators closer to the baseline case (HPV) as clearly shown in Fig. 24(d). Indeed, it can be seen as the DIP CO_2 mass flow rate fraction to evaporators (red line) better approaches the baseline line (HPV) for larger external temperatures. This means that DIP does not provide significant variation on plant behaviour when it replaces the HPV.

In Fig. 25, the impact on the refrigerating unit performances is shown with respect to the baseline (with HPV valve). In particular, despite few variations, the cooling load (Heat absorbed by working fluid across the evaporators) assume a same trend and values. Hence, keeping the same cooling operating performances, the compressor must face the same pressure ratio providing a quite equal CO_2 mass flow rate.

So, the compressor power (Fig. 25(a)) assumes comparable values for all the three cases and only small differences can be expected. Considering the ideal power recoverable, the ratio between the expander and compressor power (Expander/Compressor Power ratio) reported in Fig. 25(b) is more significant in the case of DIP expander technology which ensures a ratio close to 7 % for an external temperature of 28 °C.

The introduction of the SVRE substituting the HPV produces a benefit on COP both for a SIP and a DIP technology as it can be seen in Fig. 25(d). Indeed, being the cooling load quite the same, Fig. 25(c)

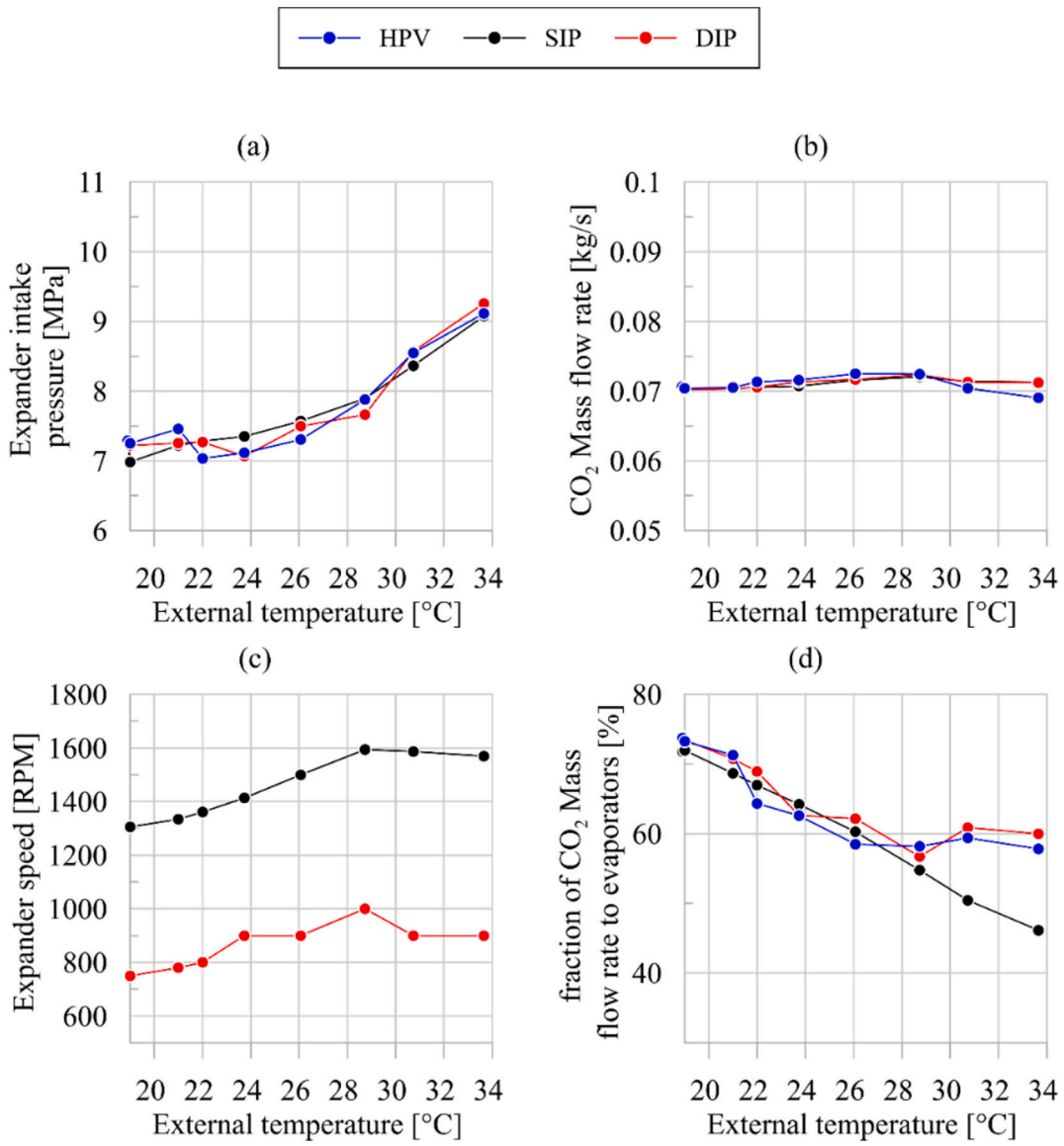

Fig. 24. Expander intake pressure (a), CO_2 mass flow rate (b), expander speed (c) and fraction of CO_2 forwarded to evaporator and SIP and DIP expander speed as function of External temperature.

considering the power recovered, shows that COP increases for all the external temperatures in case of HPV substitution with an expander. For the expander SIP technology COP benefits ranges from 2 % up to 8 % with an average value of 6 %. When the DIP technology is adopted, a larger benefit is expected with an average value of 8.5 % and a maximum value of 21 %. It could be useful to notice that from ambient temperatures between 26 °C and 34 °C COP increase is always greater than 10 %, so recovering more in terms of COP (Fig. 25(d)) when the refrigerating unit loses in terms of performances. A more detailed analysis of the results shows that also the cooling load in case of DIP expander technology (Fig. 25(c)) increases with respect to the HPV presence. The relative curve, in fact, stays almost always above that referred to HPV.

In Fig. 26 the p-h of DIP case was reported. It can be seen as the rated conditions was maintained as maximum, intermediate and minimum pressure are in the order of 8.4, 3.8 and 2.3 MPa. The most important difference is that in case of DIP installation, an enthalpy reduction is caused by the expansion taking place in DIP machine. Indeed, in HPV case a lamination transformation takes place leading to a conservation of the total enthalpy.

As final remark it can be observed that the expander has an overall efficiency close to 40 %, already considered in the previous result. The introduction of slighter material for the blades (composite compounds) will certainly improve the mechanical efficiency as the authors already verified in other applications.

4. Conclusions

In the present paper the impact of the substitution of the High-Pressure Valve (HPV) with a Sliding Rotary Vane Expander (SVRE) in a CO_2 *trans*-critical refrigeration unit was assessed thanks to a comprehensive and detailed model of the whole unit. The interest is high because the use of CO2 produces an intrinsic lower COP with respect to other refrigerating fluid, mainly when the ambient temperature increases.

The model of the refrigerating unit considers the propagative, inertial and capacitive properties of the components of the unit, being in this way a novelty in the sector, often oriented to a pure thermodynamic model. This means that the model can describe in an accurate way transient conditions and off design operation. It is suitable to be used as

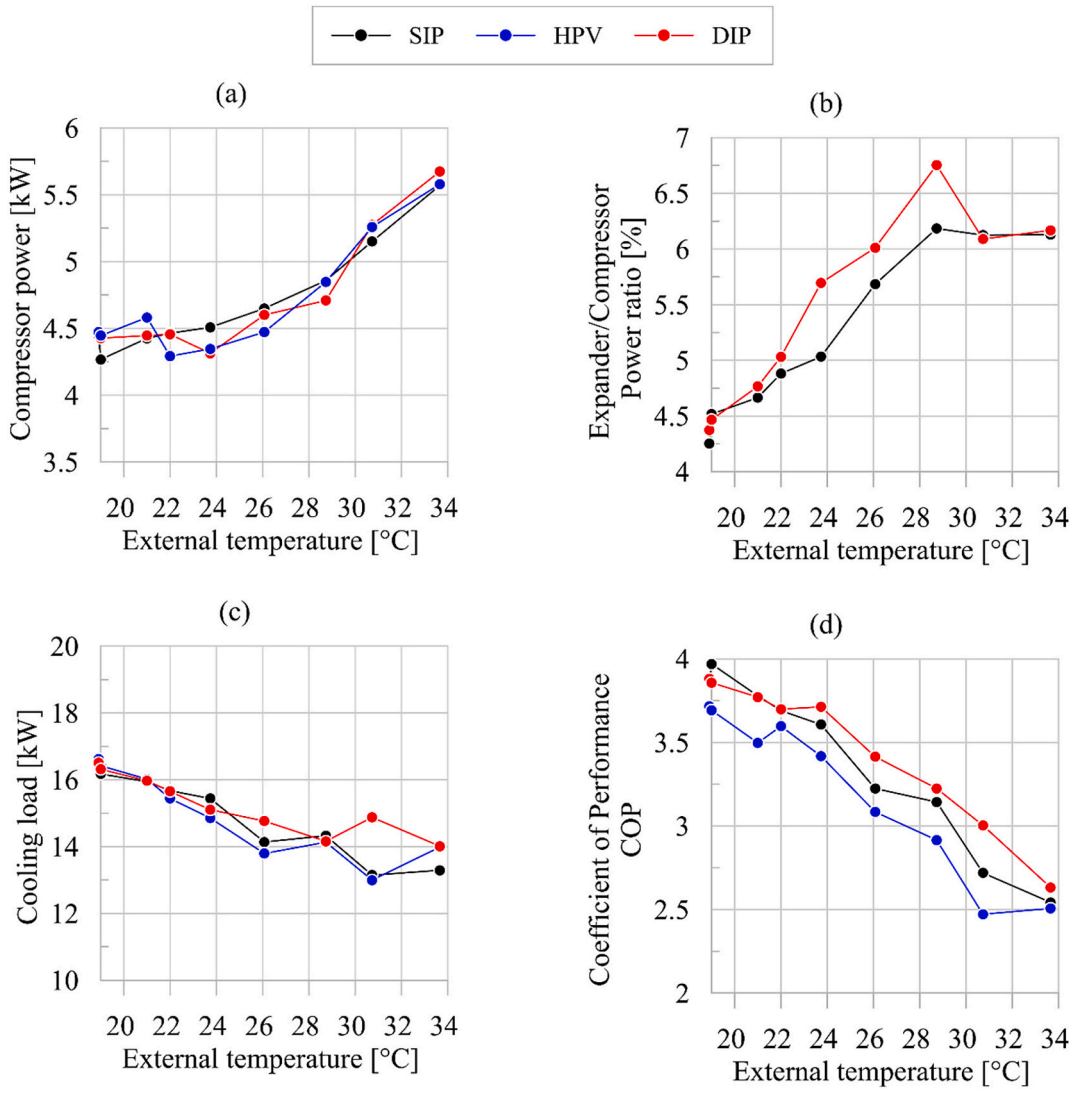

Fig. 25. Expander intake pressure (a) and CO_2 mass flow rate (b) Cooling load (c) and COP (d) a in case of HPV, SIP and DIP expander.

design tool for most critical components of the refrigeration unit for which the use of semi-empirical relationships is widely used (for instance the separator downstream the HPV). The model has been validated on the base of a wide experimental activity on a refrigeration unit having a rated cooling load of 18 kW, a maximum pressure and temperature of 8 MPa and 390 K, respectively and minimum pressure and temperature equals to 2.6 MPa and 280 K.

The design of a Sliding Vane Rotary Expander (SVRE) which replaces the High-Pressure Valve (HPV) to recover the energy usually wasted was also optimized thanks to the model. To keep the same characteristics of the refrigeration unit (cooling load, pressure values, refrigeration fluid flowrate, etc…), the model was also used to design a control strategy of the SVRE acting on the speed of revolution, as a function of the ambient temperature. In fact, the expander behaves like a "revolving valve" and the speed of revolution (considered as control variable) is a variable able to restore the pressure-flow rate response of the unit when it was managed with a HPV. Being the power recovered by the expander the paying load of the valve replacement (without neglecting the value of the externality produced by the reduction of the CO_2 emissions having reduced the power requested by the unit), an additional improvement has been presented adopting a new expander technology (the Dual Intake Port, DIP) recently developed by the authors. It introduces an additional intake port which opens after the closure of the first one.

The DIP expander replacing the HPV presents the following benefits with respect to a conventional SVRE (Single Intake Port, SIP):

- The DIP technology allows to improve the expander volumetric efficiency up to 15 % of that of the SIP technology. With DIP expander volumetric efficiency close to 0.8 was obtained ensuring a significant increase with respect to the best literature values (0.45) [37].
- The DIP technology improves the mechanical efficiency up to 15 % of that of the SIP technology.
- The DIP technology improves the global expander efficiency up to 20–25 % of that of the SIP technology. Efficiencies ranging between 0.4 and 0.32 are achieved, higher than the best literature values, [34].
- The DIP technology improves the mechanical efficiency up to 15 % of that of the SIP technology;
- The DIP technology improves the global expander efficiency up to 20–25 % of that of the SIP technology. In particular efficiency rangin between 0.4 and 0.32 are achieved, higher than the best literature values, [34].

The replacement of the HPV with a SVRE produces the following advantages:

- Both SIP and DIP expander technologies ensure to achieve a significant benefit in terms of COP with respect to the baseline case with a

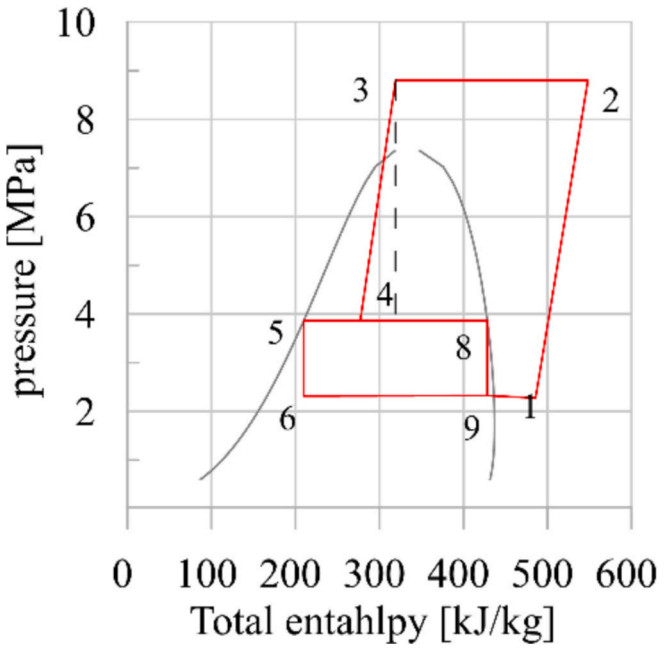

Fig. 26. P-h diagram of the refrigeration thermodynamic process in case of dip.

HPV. Indeed, an average COP increase of 6 % and 8.5 % is achieved, respectively, when the ambient temperature varies in the 18 °C-34 °C range. The benefits is higher than that achievable with other compressor type (i.e. piston as in [23]) and on the same order of those reported in literature for sliding rotary vane machine [37];

- DIP expander technology allows to reach a maximum COP increase up to 20 % for an external temperature of 28 °C. In the range 24 °C-34 °C the COP increase is never lower than 10 % for the case at hand;
- DIP expander technology operates with a revolution speed lower than 40–50 % of that requested by the SIP technology;
- Greater benefits are still achievable improving the expander performances reducing the friction between blade tip and stator surfaces experimenting composite reinforced materials for the blades which are under testing.

Besides potential further advantage related to expander installation, a deep knowledge on the impact of expander operating conditions on pressure levels is fundamental from a unit control point of view. In this paper, the attention was focused on the feasibility analysis of dual intake port vane expander which was never employed in refrigeration plant to replace high pressure valve. In this first step, the permeability theory developed by authors for ORC-based power unit, [50] was applied in refrigeration unit founding important information on what expander parameters should be adopted (speed and intake volume) to maintain the inlet and outlet pressure equal to the rated one. Indeed, as the aim is to demonstrate the benefits of DIP SVRE, the comparison was made on baseline operating conditions. Hence, having demonstrated the benefits introduced by DIP SVRE, verified the validity of permeability relation in refrigeration plant and consolidated the reliability of the model, in the next step of the present research, the expander operating conditions (revolution speed) and design parameters (intake volume) will be varied in order to investigate different operating conditions to optimize the plant performance.

CRediT authorship contribution statement

Fabio Fatigati: Writing – review & editing, Writing – original draft, Visualization, Validation, Supervision, Software, Methodology, Investigation, Formal analysis, Data curation, Conceptualization. **Roberto Cipollone:** Writing – review & editing, Writing – original draft, Visualization, Validation, Supervision, Resources, Project administration, Methodology, Funding acquisition, Formal analysis, Conceptualization.

Declaration of competing interest

The authors declare that they have no known competing financial interests or personal relationships that could have appeared to influence the work reported in this paper.

Acknowledgement

Authors are grateful to EPTA S.p.A. for the support given during the present research.

Data availability

Data will be made available on request.

References

[1] https://iifiir.org/en/fridoc/the-impact-of-the-refrigeration-sector-on-climate-change-141135.
[2] Sleiti AK, Al-Ammari WA, Al-Khawaja M, Saker AT. Experimental investigation on the performance of a novel thermo-mechanical refrigeration system driven by an expander-compressor unit. Appl Therm Eng 2022;212. https://doi.org/10.1016/j.applthermaleng.2022.118635.
[3] Zhao S, Li X, Wang L, Chang M. State-space model development and dynamic performance simulation of solar-powered single-effect LiBr-H_2O absorption chiller. Renew Energy 2025;241. https://doi.org/10.1016/j.renene.2024.122327.
[4] Wang Y, Li X, Guo Y, Dai J, Song J, He Q, et al. Thermodynamic performance and CO2 emission analysis of transcritical CO_2 two-stage compression refrigeration system with intermediate gas supplementation. Energy 2025;320. https://doi.org/10.1016/j.energy.2025.135193.
[5] Tassou SA, Ge Y, Hadawey A, Marriott D. Energy consumption and conservation in food retailing. Appl Therm Eng 2011;31:147–56. https://doi.org/10.1016/j.applthermaleng.2010.08.023.).
[6] Zou L, Liu Y, Jianlin Y. thermodynamic and environment analysis of a modified transcritical CO_2 refrigeration cycle integrated with ejector and subcooler. Int J Refrig 2025;173:123–38. https://doi.org/10.1016/j.ijrefrig.2025.02.012.
[7] Jiang J, Yang Q, Yin T, Zheng Z, Zhao Y, Liu G, Li L. Comparative thermodynamic study of CO_2 transcritical supermarket booster refrigeration system combined with vapor injection and parallel compression. Int J Refrig 2025;170:70–84. https://doi.org/10.1016/j.ijrefrig.2024.11.007.
[8] Zheng Z, Yang Q, Zhang W, Zhao Y, Liu G, Li L. Thermodynamic analysis and comparison of mechanical subcooling transcritical CO2 refrigeration system with expander and throttling valve. Case Stud Therm Eng 2025;65. https://doi.org/10.1016/j.csite.2024.105625.
[9] Abas N, Raza Kalair A, Khan N, Haider A, Saleem Z, Shoaib Saleem M. Natural and synthetic refrigerants, global warming: a review. Renew Sustain Energy Rev 2018;90:557–69. https://doi.org/10.1016/j.rser.2018.03.099.
[10] Shi R, Bai T, Wan J. Performance analysis of a dual-ejector enhanced two-stage auto-cascade refrigeration cycle for ultra-low temperature refrigeration. Appl Therm Eng 2024;240. https://doi.org/10.1016/j.applthermaleng.2023.122152.
[11] Cui Q, Gao E, Zhang Z, Zhang X. Preliminary study on the feasibility assessment of CO2 booster refrigeration systems for supermarket application in China: an energetic, economic, and environmental analysis. Energ Conver Manage 2020;225:113422. https://doi.org/10.1016/j.enconman.2020.113422.
[12] Jiang J, Yang Q, Yin T, Zheng Z, Zhao Y, Liu G, Li L. Comparative thermodynamic study of CO2 transcritical supermarket booster refrigeration system combined with vapor injection and parallel compression. Int J Refrig 2025;170:70–84. https://doi.org/10.1016/j.ijrefrig.2024.11.007.
[13] Li Y, Deng J. Numerical investigation on the performance of transcritical CO2 two-phase ejector with a novel non-equilibrium CFD model. Energy 2022;238(Part C). https://doi.org/10.1016/j.energy.2021.121995.
[14] Bai T, Shi R, Jianlin Y. Thermodynamic performance evaluation of an ejector-enhanced transcritical CO2 parallel compression refrigeration cycle. Int J Refrig 2023;149:49–61. https://doi.org/10.1016/j.ijrefrig.2022.12.014.
[15] Murthy AA, Norris S, Subiantoro A. Experimental analysis of a refurbished heat pump refrigeration system with a four-intersecting-vane expander. Appl Therm Eng 2021;183(Part 1). https://doi.org/10.1016/j.applthermaleng.2020.116209.
[16] Nebot-Andrés L, Calleja-Anta D, Sánchez D, Cabello R, Llopis R. Experimental assessment of dedicated and integrated mechanical subcooling systems vs parallel compression in transcritical CO_2 refrigeration plants. Energ Conver Manage 2022;252. https://doi.org/10.1016/j.enconman.2021.115051.
[17] Liu S, Bai T, Wei Y, Jianlin Y. Performance analysis of a modified ejector-enhanced auto-cascade refrigeration cycle. Energy 2023;265. https://doi.org/10.1016/j.energy.2022.126334.
[18] Wen Z, Bai T, Wan J. Thermodynamic analysis of a modified transcritical CO2 two-stage compression dual-temperature refrigeration cycle with an ejector. Appl

Therm Eng 2024;257(Part B). https://doi.org/10.1016/j.applthermaleng.2024.124383.
[19] Liu Y, Liu J, Jianlin Y. Theoretical analysis on a novel two-stage compression transcritical CO_2 dual-evaporator refrigeration cycle with an ejector. Int J Refrig 2020;119:268–75. https://doi.org/10.1016/j.ijrefrig.2020.08.002.
[20] Yuheng D, Tian G, Pekris M. A comprehensive review of micro-scale expanders for carbon dioxide related power and refrigeration cycles. Appl Therm Eng 2022;201 (Part A). https://doi.org/10.1016/j.applthermaleng.2021.117722.
[21] Imran M, Usman M, Park B-S, Lee D-H. Volumetric expanders for low grade heat and waste heat recovery applications. Renew Sustain Energy Rev 2016;57: 1090–109. https://doi.org/10.1016/j.rser.2015.12.139.
[22] Zhang X, Yujie X, Zhou X, Zhang Y, Li W, Zuo Z, Guo H, Huang Y, Chen H. A near-isothermal expander for isothermal compressed air energy storage system. Appl Energy 2018;225:955–64. https://doi.org/10.1016/j.apenergy.2018.04.055.
[23] Ferrara G, Ferrari L, Fiaschi D, Galoppi G, Karellas S, Secchi R, Tempesti D. Energy recovery by means of a radial piston expander in a CO_2 refrigeration system. Int J Refrig 2016;72:147–55. https://doi.org/10.1016/j.ijrefrig.2016.07.014.
[24] Shen L, Wang W, Yuting W, Cheng L, Lei B, Zhi R, Ma C. Theoretical and experimental analyses of the internal leakage in single-screw expanders. Int J Refrig 2018;86:273–81. https://doi.org/10.1016/j.ijrefrig.2017.10.037.
[25] Kovačević A, Stošić N, Smith IK. Numerical simulation of combined screw compressor–expander machines for use in high pressure refrigeration systems. Simul Model Pract Theory 2006;14(8):1143–54. https://doi.org/10.1016/j.simpat.2006.09.004.
[26] M. Fukuta, T. Yanagisawa, O. Kosuda, Y. Ogi, Purdue e-Pubs Performance of Scroll Expander for CO2 Refrigeration Cycle Performance of Scroll expander for CO 2 Refrigeration Cycle, n.d. https://docs.lib.purdue.edu/icec (accessed October 20, 2020).
[27] H. Kohsokabe, H. Masaki, K. Hitachi, K. Tojo, H. Appliances, M. Matsunaga, S. Nakayama, M. Koyama, K. Toj0, S.N. Yama, Performance Characteristics of Scroll Expander for CO2 Refrigeration Cycles, 2008. https://docs.lib.purdue.edu/icec/1847 (accessed August 31, 2020).
[28] Hiwata A, Ikeda A, Morimoto T, Kosuda O, Matsui M. Axial and radial force control for a co2 scroll expander. HVAC R Res 2009;15(4):759–70. https://doi.org/10.1080/10789669.2009.10390862.
[29] Fukuta M, Anzai F, Motozawa M, Terawaki H, Yanagisawa T. Performance of radial piston type reciprocating expander for CO_2 refrigeration cycle. Int J Refrig 2014; 42:48–56. https://doi.org/10.1016/j.ijrefrig.2014.02.005.
[30] Fukuta M, Adachi M, Yanagisawa T. Transcritical leakage flow in CO2 expander. In: in: International Symposium on Next Generation Air Conditioning and Refrigeration Technology; 2010. p. 1–8.
[31] B. Yang, X. Peng, S. Sun, B. Guo, Z. Xing, Study of a rotary vane expander for the trans critical CO 2 (2009) 673–688. cycle part I: experimental investigation, HVAC&R Res. 15 (4).
[32] X. Jia, B. Zhang, B. Yang, X. Peng, Study of a rotary vane expander for the transcritical CO 2 689–709. 2 cycle part II: theoretical modelling, HVAC&R Res. 15 (4) (2009).
[33] Yang B, Peng X, He Z, Guo B, Xing Z. Experimental investigation on the internal working process of a CO2 rotary vane expander. Appl Therm Eng 2009;29(11–12): 2289–96. https://doi.org/10.1016/j.applthermaleng.2008.11.023.
[34] Jia X, Zhang B, Yang B, Peng X. Improved rotary vane expander for transcritical CO cycle by introducing high pressure gas into the vane slots. Int J Refrig 2011;34(3): 732–41.
[35] Fabris F, Artuso P, Marinetti S, Minetto S, Rossetti A. Dynamic modelling of a CO2 transport refrigeration unit with multiple configurations. Appl Therm Eng 2021; 189. https://doi.org/10.1016/j.applthermaleng.2021.116749.
[36] Subiantoro A, Ooi KT. Economic analysis of the application of expanders in medium scale air-conditioners with conventional refrigerants. R1234yf and CO Int J Refrig 2013;36(5):1472–82.
[37] Murthy AA, Subiantoro A, Norris S, Fukuta M. A review on expanders and their performance in vapour compression refrigeration systems. Int J Refrig 2019;106: 427–46. https://doi.org/10.1016/j.ijrefrig.2019.06.019.
[38] Li W, Korolija I, Tang R, Mumovic D. High-fidelity model development of CO2 booster refrigeration systems in supermarkets using field measurements. Int J Refrig 2025;169:152–65. https://doi.org/10.1016/j.ijrefrig.2024.10.025.
[39] Shu Y, Yan J. Thermodynamic modeling and performance optimization of transcritical CO2 dual-evaporator refrigeration system enhanced with ejectors. Appl Therm Eng 2024;249. https://doi.org/10.1016/j.applthermaleng.2024.123433.
[40] Wang M, Zhao Y, Cao F, Gaoxuan B, Wang Z. Simulation study on a novel vane-type expander with internal two-stage expansion process for R-410A refrigeration system. Int J Refrig 2012;35(4):757–71. https://doi.org/10.1016/j.ijrefrig.2011.11.014.
[41] Fatigati F, Di Battista D, Carapellucci R, Cipollone R. Model-based improvement of a trans-critical CO2 refrigeration plant (2024). J Phys: Conference Series 2024; 2893(1):012114. https://doi.org/10.1088/1742-6596/2893/1/012114.
[42] Fatigati F, Di Bartolomeo M, Di Battista D, Cipollone R. A dual-intake-port technology as a design option for a Sliding Vane Rotary Expander of small-scale ORC-based power units. Energ Conver Manage 2020;209. https://doi.org/10.1016/j.enconman.2020.112646.
[43] Fatigati F, Di Bartolomeo M, Cipollone R. Dual intake rotary vane expander technology: experimental and theoretical assessment. Energy Conversion and Manage 2019;186:156–67. https://doi.org/10.1016/j.enconman.2019.02.026.
[44] https://www.bitzer.de/websoftware/calculate/HHK/?tab=techData.
[45] Ismail Tosun, 4 - EVALUATION OF TRANSFER COEFFICIENTS: ENGINEERING CORRELATIONS, Editor(s): Ismail Tosun, Modeling in Transport Phenomena (Second Edition), Elsevier Science B.V., 2007, Pages 59-115, ISBN 9780444530219.
[46] Boissieux X, Heikal MR, Johns RA. Two-phase heat transfer coefficients of three HFC refrigerants inside a horizontal smooth tube, part II: condensation. Int J Refrig 2000;23(5).
[47] Lichtarowicz A, Duggins R, Markland E. Discharge coefficients for incompressible non-cavitating flow through long orifices. J Mech Eng Sci 2006;7(2):210–9.
[48] Martínez-Ángeles M, Petruzziello F, Nebot-Andrés L, Aprea C, Maiorino A, Llopis R. New phase separation phenomena in refrigeration plants working with CO_2-based mixtures. Experimental approach. Int J Refrig 2025;172:75–86. https://doi.org/10.1016/j.ijrefrig.2025.01.032.
[49] Hazarika MM, Ramgopal M, Bhattacharyya S, Doménech RL. Role of receiver on the performance of a transcritical CO_2 based air-conditioning unit with single-stage and two-stage expansion. Sci Technol Built Environ 2021;27(5):1–28. https://doi.org/10.1080/23744731.2021.1902189.
[50] Fatigati F, Di Bartolomeo M, Cipollone R. On the effects of leakages in sliding rotary vane expanders. Energy 2020;192. https://doi.org/10.1016/j.energy.2019.116721.
[51] Fatigati F, Di Giovine G, Cipollone R. Feasibility assessment of a dual intake-port scroll expander operating in an ORC-based power unit. Energies 2022;15, no. 3: 770. https://doi.org/10.3390/en15030770.